Construction and Building Materials 489 (2025) 142174

Contents lists available at ScienceDirect

Construction and Building Materials

journal homepage: www.elsevier.com/locate/conbuildmat

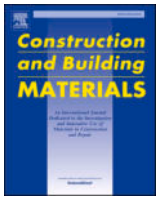

Experimental in-situ characterisation of the damping properties of road pavements

G. Loi [a,*], M.C. Porcu [b], F. Maltinti [b], M. Coni [b], F. Aymerich [a]

[a] Department of Mechanical, Chemical and Materials Engineering, University of Cagliari, Piazza d'Armi, Cagliari 09123, Italy
[b] Department of Civil, Environmental Engineering and Architecture, University of Cagliari, Piazza d'Armi, Cagliari 09123, Italy

ARTICLE INFO

Keywords:
In-Situ Tests
Damping Characterisation
Road Pavements

ABSTRACT

Vibrations induced by tyre/pavement interaction may be of concern for the underlying structure and, due to propagation of waves, for surroundings buildings and facilities. In addition, they may cause discomfort to drivers and passengers of vehicles, as well as traffic noise pollution. Improving damping properties of roads may mitigate most of the harmful traffic-induced effects. Nevertheless, the evaluation of damping properties of road systems is still an open issue. The present paper aims to contribute to this matter by assessing the effectiveness of two procedures for the in-situ characterisation of road pavement damping. The first procedure (MDPE-SD) evaluates the damping properties of physical vibration modes by means of a modal parameter identification algorithm used in association with stabilisation diagrams. The second procedure (CWT-ED) applies a wavelet transform for frequency decoupling and estimates damping by evaluating the rate of signal decay. In-situ tests, in which an instrumented hammer and an accelerometer were used respectively to apply an impact load and to measure the vibration response, were conducted on flexible and rigid pavements. The reliability of the two experimental procedures was assessed and compared by examining the damping ratios estimated for the two pavements at different frequencies and for different excitation and sensing locations. The investigation indicated that the spectral response of the pavements was characterised by multiple closely spaced modes, thus affecting the reliability of their identification through the MDPE algorithm. The analyses also showed that the damping ratios provided by the MDPE-SD procedure may be greatly affected by the choice of the excitation and sensing locations. In contrast, the CWT-ED procedure was much more robust, at any of the frequencies considered for the two pavement systems tested, to changes in the excitation and sensing sites, thus highlighting its superior capability to estimate the damping properties of road pavements.

1. Introduction

1.1. Background and aim of the study

Vibrations induced by vehicles on road pavements may generate various detrimental effects, such as an increase in environmental noise, a reduction in drivers' comfort, as well as potentially threatening impacts on underlying and surrounding structures.

According to the WHO Regional Office for Europe [1], road traffic noise pollution is the second biggest health risk after air pollution. Tyre-pavement interaction, especially from vehicles moving at medium to high speed, is the dominant source of traffic noise [2]. In addition, vibrations induced by tyre-pavement interaction may cause discomfort for drivers and passengers of road vehicles, which can be particularly hazardous for certain categories of workers, such as public transport drivers and operators [3,4]. Road traffic-induced vibrations are also of concern for both the underlying pavement structure and overlying constructions. The dynamic characteristics of asphalt pavements, particularly damping properties, were found to significantly influence the response of bridges and footbridges [5–7]. Due to the propagation of waves both in the ground and in the air, traffic/road interaction may also induce vibrations in the surrounding civil engineering facilities, which may seriously affect lighter non-structural parts and fragile internal contents of buildings [8]. Particular attention is paid to historical monuments, where frescoes and precious furnishings are present [9,10] as well as to sensitive buildings like hospitals, research labs and high-tech industries [11]. It should finally be mentioned that the quality of the road surface has a direct influence on vehicle durability and

* Corresponding author.
E-mail address: gabriela.loi@unica.it (G. Loi).

https://doi.org/10.1016/j.conbuildmat.2025.142174
Received 20 March 2025; Received in revised form 3 June 2025; Accepted 6 June 2025
Available online 12 June 2025
0950-0618/© 2025 The Authors. Published by Elsevier Ltd. This is an open access article under the CC BY license (http://creativecommons.org/licenses/by/4.0/).

maintenance [12].

Most of the traffic-induced effects could be mitigated by improving the characteristics of the road pavement such as surface texture and roughness, void content, and viscoelastic (stiffness and damping) properties of materials [13]. Among these properties, damping plays a key role, as shown, for example, by current research on the development of quieter [2,14] or anti-vibration pavement systems with damping layers [11]. The inclusion of rubberized high-porous damping layers and the optimization of the asphalt mixture have been found to improve the dissipative and noise-absorption properties of asphalt mixtures [15–17]. The key role of damping in minimizing vibrations brought on by traffic in recycled asphalt pavements is also recognized [18].

The knowledge of the dissipative properties of road pavements is therefore of the utmost importance both to assess the performance of existing roads and to design new road structures. In the vast majority of the existing research on the subject, the global behaviour of road pavements is simulated using analytical or finite element models based on the elastic, inertial and dissipative properties of the individual layers [19,20]. In numerical dynamic analyses, Falling Weight Deflectometer (FWD) tests are often simulated [17,19–21] in order to estimate the structural and damping properties of the individual pavement layers through back-calculation methods, which are based on matching numerical and experimental time histories of surface deflection data. Flexible pavements are usually modelled with layers extending indefinitely in the horizontal directions and supported by a Winkler foundation where springs are combined with dashpots to simulate damping effects [19]. As an example, a theoretical model was recently developed in [22] to study the problem of back-calculation of layer properties of asphalt pavements under an impact load. The study was based on a wave propagation approach and a complex model to describe the viscoelastic behaviour of a multilayered medium assumed to be made of linear, homogeneous and isotropic materials. It is worth noting how these models are typically validated through qualitative comparisons between simulated and experimentally measured deflection-time histories, while no specific evaluation is performed in terms of the global energy dissipation capacity of the examined pavements.

Although the existing literature demonstrates the crucial importance of the energy dissipation efficiency of road pavements, little specific research has been conducted on possible strategies for in situ experimental characterisation of the damping properties of pavement systems, which remains an open issue worthy of further exploration. The aim of the present study is to explore and test experimental methodologies that can be easily implemented in the field for the in-situ evaluation of the global dissipative properties of road pavements. The damping behaviour of the pavements was characterised in terms of their capacity to dissipate vibrational energy induced by dynamic loads, resulting in an attenuation of surface vibration amplitude over time. The widely used damping ratio ξ was chosen as the parameter to represent this dissipative behaviour in a quantitative and reproducible way. A key aspect of the proposed methodologies is their ability to assess the dependence of damping ratios on vibration frequency. It must be clarified that the study conducted was experimental in nature and that the proposed analyses do not rely on assumptions regarding the constitutive laws of individual pavement layers or the physical mechanisms governing the damping behaviour.

1.2. Damping properties of linear dynamic models

Energy dissipation occurs during vibrations of civil constructions due to various mechanisms that are inherently inelastic and difficult to be fully identified and described (e.g., internal and external friction, viscous dissipation, thermal effects due to repeated elastic straining, opening and closing of microcracks in concrete) [23]. An idealized way to account for dissipative effects in linear dynamic systems is that of considering equivalent viscous damping. To this purpose, viscous dampers (dashpots) are introduced in the mechanical models, by assuming that they can dissipate the same energy dissipated by the many mechanisms acting in the real structure. When a single degree of freedom (SDOF) system with mass m and stiffness k is considered, the dashpot produces a dissipative force $F_d = -c\dot{u}(t)$, proportional (and opposite) to the velocity $\dot{u}(t)$ of the mass through a constant damping coefficient c. The nondimensional damping ratio ξ given by

$$\xi = \frac{c}{2m\omega} \tag{1}$$

is usually introduced in dynamic studies. It depends on the natural angular frequency $\omega = \sqrt{k/m}$ of the SDOF system [23]. Civil constructions are typically underdamped systems ($\xi < 1$), which oscillate about the equilibrium position under free motion, gradually dissipating vibrational energy and attenuating displacement amplitude.

For multi-degree of freedom (MDOF) systems, the modal damping ratio ξ_i at i-th angular frequency ω_i is defined as:

$$\xi_i = \frac{c_i}{2\,\omega_i\,\{\psi^{(i)}\}^t\,[m]\,\{\psi^{(i)}\}} \tag{2}$$

where c_i is the coefficient of the i-th dashpot and $\{\psi^{(i)}\}$ is the shape vector of the i-th mode. Once the mass $[m]$ and stiffness $[k]$ matrices of the MDOF system are given, natural frequencies ω_i and mode shapes $\{\psi^{(i)}\}$ can be straightforwardly found by solving the eigenvalue and eigenvector problem $\left([k]-\omega_i^2[k]\right)\{\psi\} = \{0\}$. In contrast, damping ratios cannot be directly evaluated from geometrical, mechanical, and inertial properties of the structure, since they depend on the damping coefficients c_i, which are generally unknown quantities. Experimental tests are thus needed to evaluate the damping ratios of existing systems.

A popular approximate way to obtain the damping matrix $[c]$ of a MDOF system (which is made of the damping coefficients c_i) is the Rayleigh method, which assumes that $[c]$ is given by the sum of the mass-proportional damping $\alpha[m]$ and the stiffness proportional damping $\beta[k]$ [23]. The Rayleigh method is often exploited in numerical simulations of road pavement systems [24,25], where each layer of the pavement system is assigned a Rayleigh damping matrix. However, to obtain the Rayleigh damping matrix, the values of the proportional coefficients α and β should be preliminarily determined. It can be shown that the values of parameters α and β can be determined by solving the following algebraic system [23]:

$$\begin{cases} \xi_j = \dfrac{\alpha}{2\,\omega_j} + \dfrac{\beta\,\omega_j}{2} \\ \xi_k = \dfrac{\alpha}{2\,\omega_k} + \dfrac{\beta\,\omega_k}{2} \end{cases} \tag{3}$$

where ω_j and ω_k are the eigenfrequencies relevant to modes j and k, while ξ_j and ξ_k are the relevant damping ratios. While eigenfrequencies ω_j and ω_k can be easily extracted from the numerical model, damping ratios ξ_j and ξ_k should be determined from experimental tests on the real structure. Typically, the first two natural modes are considered to solve system (3), and the assumption of a frequency-independent damping ratio is often made. It must be noted, however, that the assumption of damping ratios being independent of the vibration frequency is generally not appropriate for highly heterogeneous systems such as road pavements. Furthermore, in-situ evaluations of the overall dissipative capacity of real pavement systems are still required to tune and validate models built on the basis of properties assigned at the level of the individual layers.

1.3. Experimental characterisation of damping properties

The many techniques used to extract the modal dynamic properties of structural systems may be distinguished into three main categories: time-domain methods, frequency-domain methods and time-frequency-domain methods [26,27].

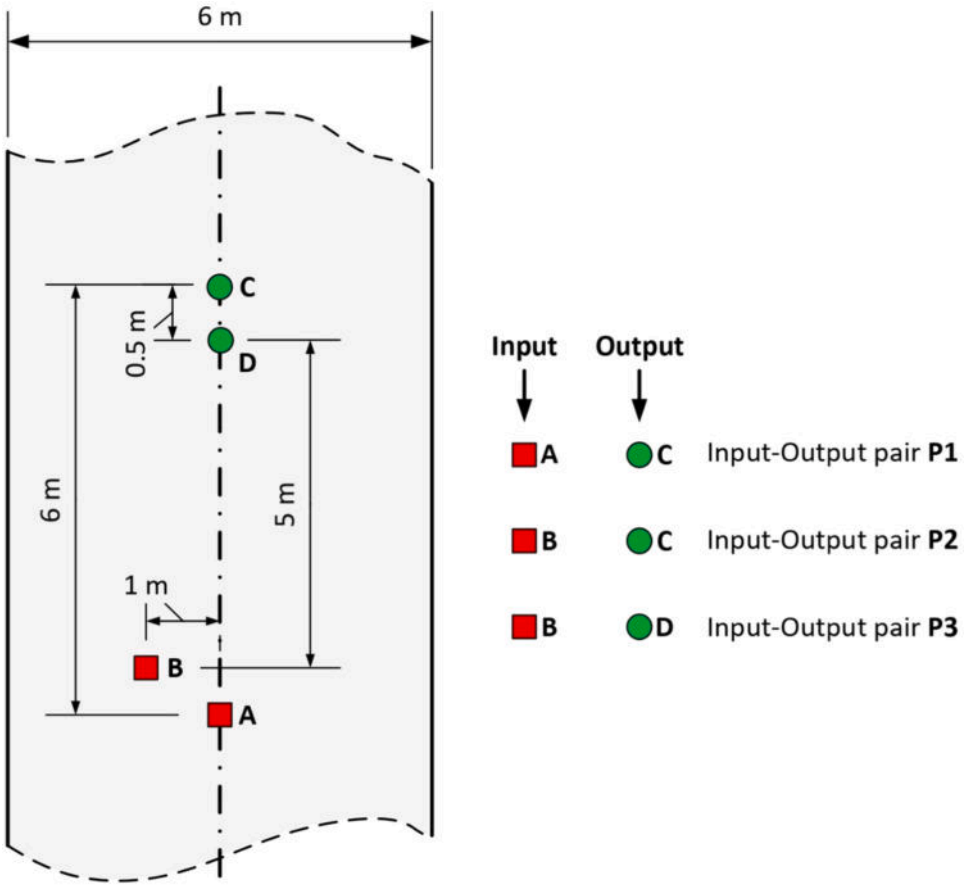

Fig. 1. Input-output pairs selected for the tests on the flexible road pavements.

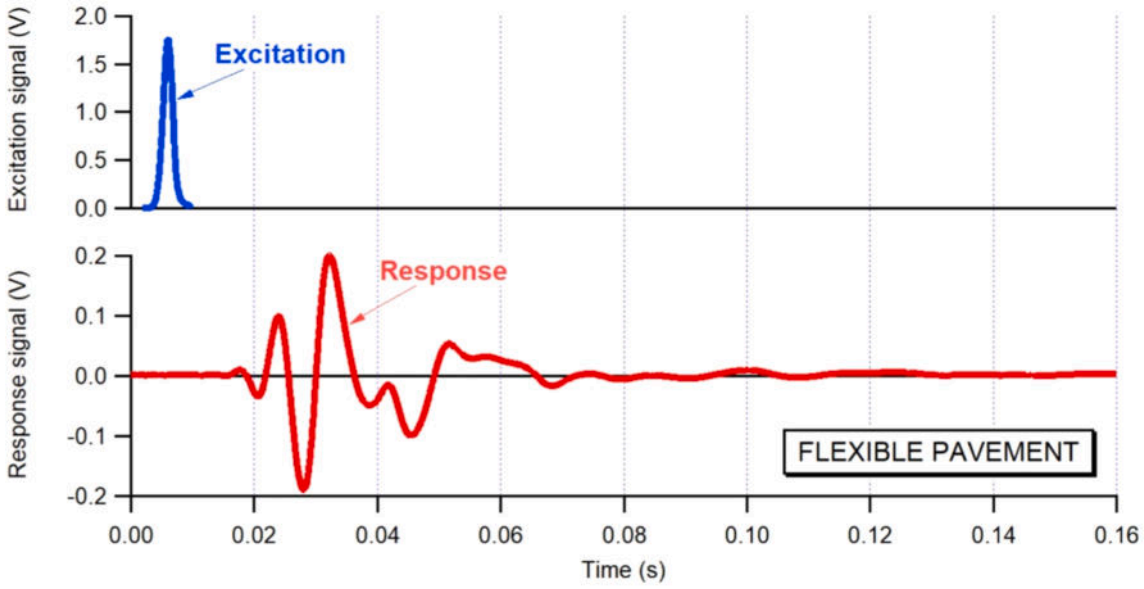

Fig. 2. Typical excitation and vibration signals acquired from measurements on the flexible pavement from the input-output pair P1.

Most time-domain methods [28,29] are based on the analysis of the decay over time of the system's free oscillation, which can be expressed as a sum of the contributions from all modes of vibration. The free oscillation of the system can be induced by an impulse load or by the abrupt cut-off of continuous excitation. When the response of the system is dominated by a single mode, the damping ratio can be estimated by measuring the logarithmic decay of successive peaks in the time response. More advanced approaches, based on fitting procedures (e.g., Prony's or Least Squares Complex Exponential techniques) or eigenvalue decomposition (such as the Ibrahim Time Domain method), are required to extract the damping ratios of individual modes in more realistic multi-mode structural systems. Alternative time-domain

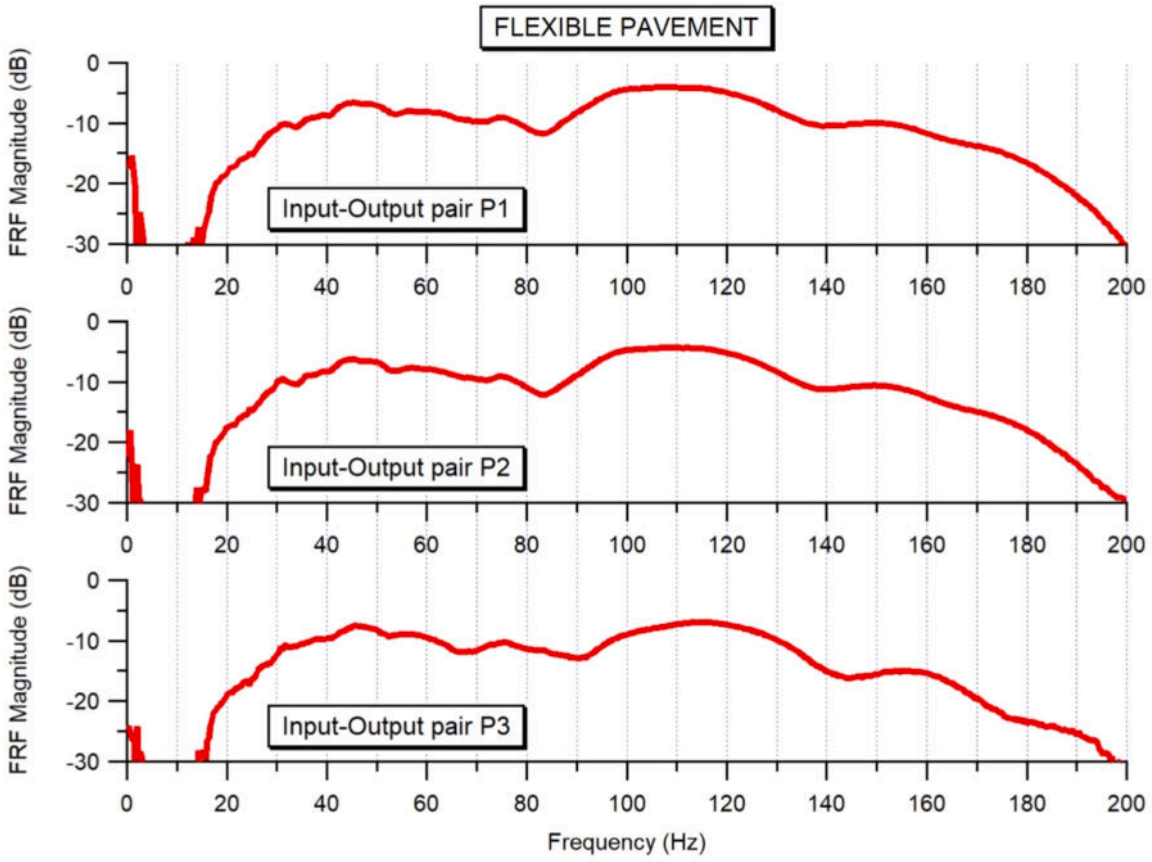

Fig. 3. FRFs of the flexible pavement acquired from the three examined input-output pairs.

techniques, always based on the assumption of a single degree of freedom, involve measuring the response of the system under steady-state harmonic excitation to evaluate the complex modulus, which provides information on both the elastic and dissipated energy in each cycle. In particular, the phase lag between the excitation and the response is proportional to the energy dissipated and can be related to the damping ratio of the system. All time-domain methods, however, typically rely on the assumption that modes are well separated and can be analysed independently. In structural systems with heavily coupled vibration modes, the accuracy and reliability of these methods are greatly reduced, and in some cases, they cannot be applied at all.

Frequency domain techniques rely on analysing the frequency response function (FRF) of the system, with the classical Half Power bandwidth and Circle Fit methods being widely used for damping estimation in modal analysis [28,29]. However, while these methods may be adequate for systems with well-defined and isolated resonance peaks, they are not as effective for complex or heavily damped systems. Suitable for systems with interacting modes, frequency-based methods employ modal identification procedures that account for the presence of multiple modes over a range of predefined frequencies. In the past decades, many identification algorithms (e.g., the Rational Fraction Polynomial Algorithm, the Direct Modal Parameter Estimation, and the Dual Fitting Method, to cite just a few), typically based on a representation of the FRF through a predefined number of real or complex orthogonal polynomials, have been proposed and applied for the identification of modal properties [28–31]. These algorithms estimate the damping ratios of the individual modes by identifying the poles of the FRF polynomial function, which are directly related to the natural frequencies and damping properties of the associated vibration modes. It should be noted that the identification of modal parameters may become particularly difficult in the presence of overlapping and heavily damped modes [32].

Methods based on time-frequency analysis simultaneously analyse the characteristics of the vibration signal in both time and frequency domains. Several techniques relying on a number of numerical approaches have been proposed and exploited to investigate the damping properties of structural systems [26,33–41]. In particular, modal decoupling strategies where the response of the system is decomposed into modal functions have been proposed in recent years for damping estimation [33,34,42,43]. The basic approach [33], consists of representing the response of the system as the superposition of a finite number of modal functions with different frequencies or scales and estimating the damping characteristics of the individual modes by analysing the amplitude decay with time. Among the various mathematical tools for signal decomposition, the Continuous Wavelet Transform (CWT) is especially suited for these analyses, due to its capability to extract detailed multiresolution time-frequency (scale) information from transient signals. Procedures for the estimation of damping at different frequencies using modal decomposition by continuous wavelet transforms are discussed, for example, in [33,44,45], with reference to simulated or real data from simple laboratory-scale systems such as beams and trusses, or large scale systems such as buildings [46], towers [47] or bridges [46,34].

1.4. Experimental characterisation of damping in road pavements

The summary outlined in the previous paragraphs indicates that identifying damping properties can be extremely challenging in systems such as road pavements, which, due to their complex and highly heterogeneous structure, exhibit a dynamic response involving closely spaced and overlapping modes. This, along with the difficulty in applying a controlled steady state excitation as required by some methods, explains why very few investigations have been conducted in the field to characterise the in-situ damping characteristics of pavement

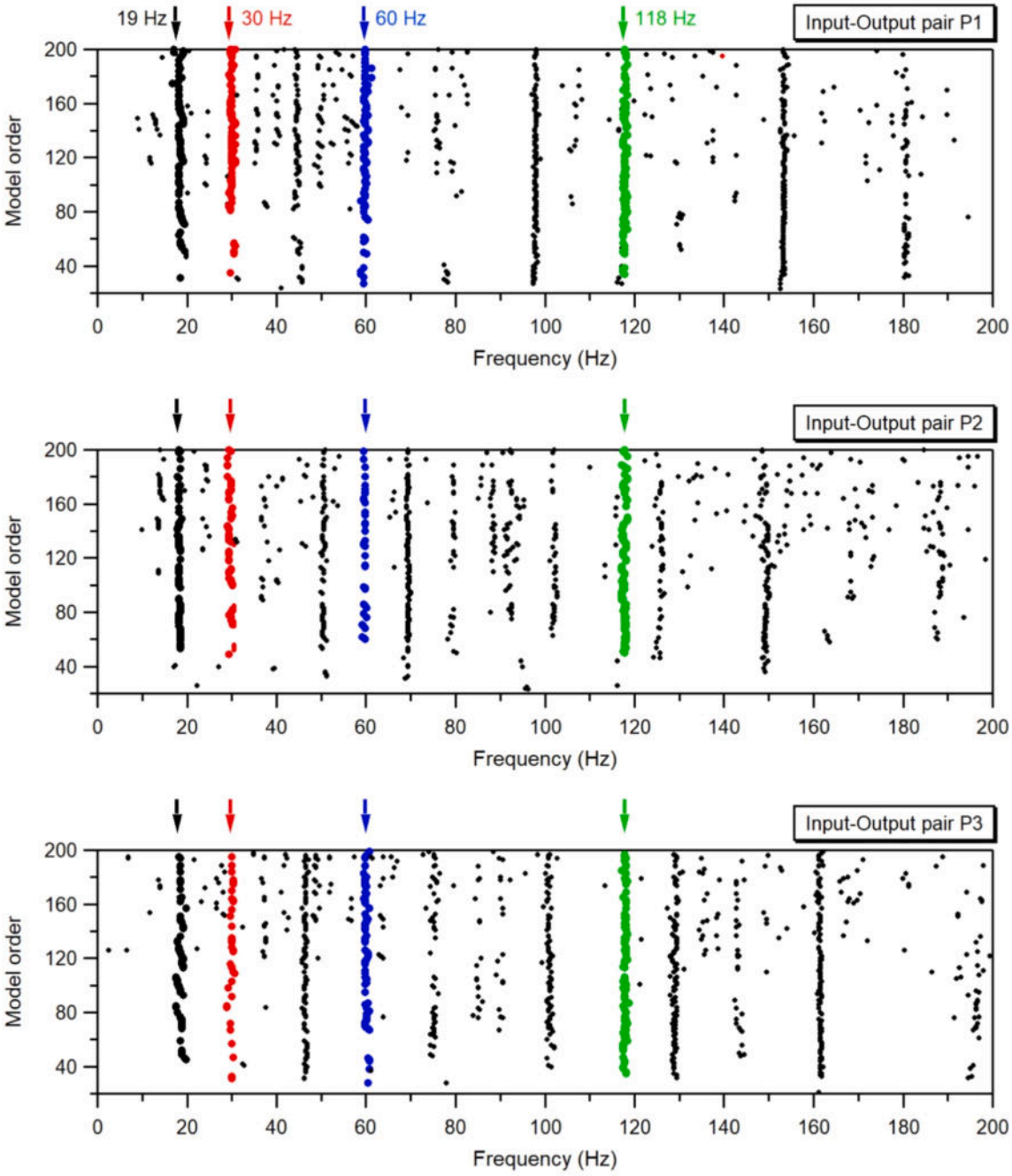

Fig. 4. Stabilisation diagrams of the modal response of the flexible pavement constructed using the DMPE algorithm for the three examined input-output pairs.

systems. In contrast, many well-established laboratory procedures, some of which are adopted by international standards, are available to evaluate damping in materials used for pavement construction. Free vibration tests, for example, were performed on cantilever beams in [48] to compare the dissipative characteristics of rubberized asphalt binders. The logarithmic decrement technique was used to calculate the damping ratios of the materials at the first natural frequency of the clamped beam. Dynamic tests were carried out in [15,16,49,50] on small cylindrical specimens subjected to compressive sinusoidal loading to determine the phase angles of asphalt mixtures as a function of frequency, in accordance with the AASHTO guidelines [51]. Similarly, the dissipative properties of asphalt mixtures were characterised by Hasheminejad and coworkers by measuring the phase angles during tests conducted on prismatic beams under dynamic bending loads [52]. In particular, asphalt specimens were impacted by a hammer, and the FRF of the system was analysed to determine the damping properties using the half-power bandwidth technique. A similar procedure was applied also in [18] to find damping ratios of cylindrical samples of recycled asphalt mixtures. Frequency domain analyses were employed in [53,54] to evaluate the damping properties of bituminous mixtures used in road surface layers. The tests were performed on rectangular slabs and cylindrical samples, excited using an instrumented impact hammer. The half-power bandwidth technique was applied to the measured FRFs to determine the damping ratios at the natural frequencies of the examined structures. Torsional shear vibrations on laboratory samples of porous asphalt mixtures were performed in [17] to assess the effects of rubble particle content on the damping performance and dynamic shear modulus. According to laboratory tests, the damping ratios of materials used in the layers constituting road pavements cover a wide range of values, from 4 % to more than 40 %, depending on the material and

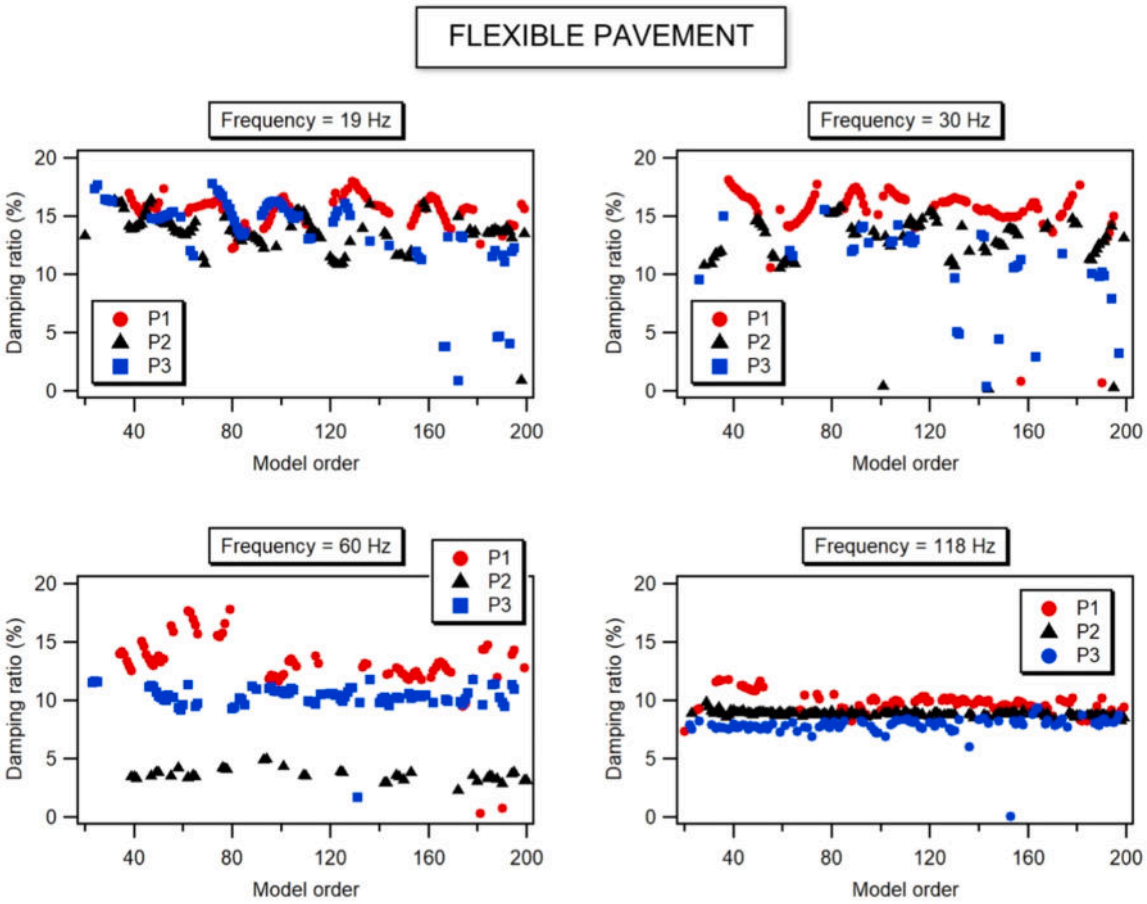

Fig. 5. Damping ratios of the flexible pavement estimated at 19 Hz, 30 Hz, 60 Hz, and 118 Hz using the DMPE-SD algorithm for the three examined input-output pairs.

temperature.

It must, however, be remarked that the dissipative behaviour of a road pavement results from the combination of multiple factors [16,55], which, in addition to the damping properties of the individual layers, include constraint conditions and geometric characteristics, interaction between pavement layers, subgrade influence, thermal and moisture effects, as well as damage mechanisms such as cracking and rutting. All these factors play a significant role in determining the final damping performance of the whole pavement structure, which is therefore extremely difficult, if not impossible, to predict accurately based solely on the dissipative properties of the specific layers measured in laboratory tests. In-situ measurements, which inherently account for the cumulative effects of the various physical phenomena, are therefore necessary for quantitative estimates of the damping properties of road pavement systems. These overall damping properties are essential for the development, calibration, and validation of models based on the damping characteristics of the constituent layers, and their knowledge can be extremely useful for verifying design requirements, monitoring pavement conditions, and comparing alternative pavement configurations. In spite of this need, only a few investigations [16,54,56–58] have focused on experimental methodologies that can be applied in the field to characterise the actual damping behaviour of road pavement systems.

A time-domain procedure was used in [58], to obtain static and dissipative properties of pavement layers under FWD impact. The method, based on a layered visco-elastic model of the pavement and on the Newton algorithm, is applied to back-calculate the damping ratios of base and subgrade layers by matching the peak deflections and the time lag between the FWD load and the deflection measured at different positions of the pavement. The damping ratios of the layers were assumed to be independent of frequency. Proper parameter tuning allows the model to accurately predict both peak deflections and time lags of field data, but a large difference is observed between numerical and measured data in terms of deflection attenuation over time, thus clearly indicating that the model is not capable of correctly capturing the dissipative response of the whole pavement system.

A comparison between time histories obtained in situ from FWD tests and from finite element simulations is presented in [16], where a method is proposed to calculate the frequency independent Rayleigh damping parameters of the various layers of flexible pavements. Neither model predictions nor experimental values extracted from the field experimental data are, however, provided for the overall damping response of the examined pavement.

Uglova and Tiraturyan [56] examined the damping performances of road pavements by analysing the attenuation of elastic waves generated by a dynamic load. The pavement was excited by impacts applied using a FWD and the time-histories of vertical displacements were acquired at different distances from the impact site. The authors suggest estimating the damping ratio of the road pavement by evaluating the decay with distance of the peak values of the measured displacements. Unfortunately, no values of estimated damping ratios are reported in the paper. A serious limitation of the chosen approach is that it does not account for the decay of the wave amplitude due to geometric spreading as the waves move out from source. In addition, the proposed damping identification analysis is not capable of providing information on the dependence of damping properties on the vibration frequency.

Some data related to the assessment of the dissipative performances of a composite road pavement obtained through a monitoring system consisting of embedded accelerometers are presented in [57]. The

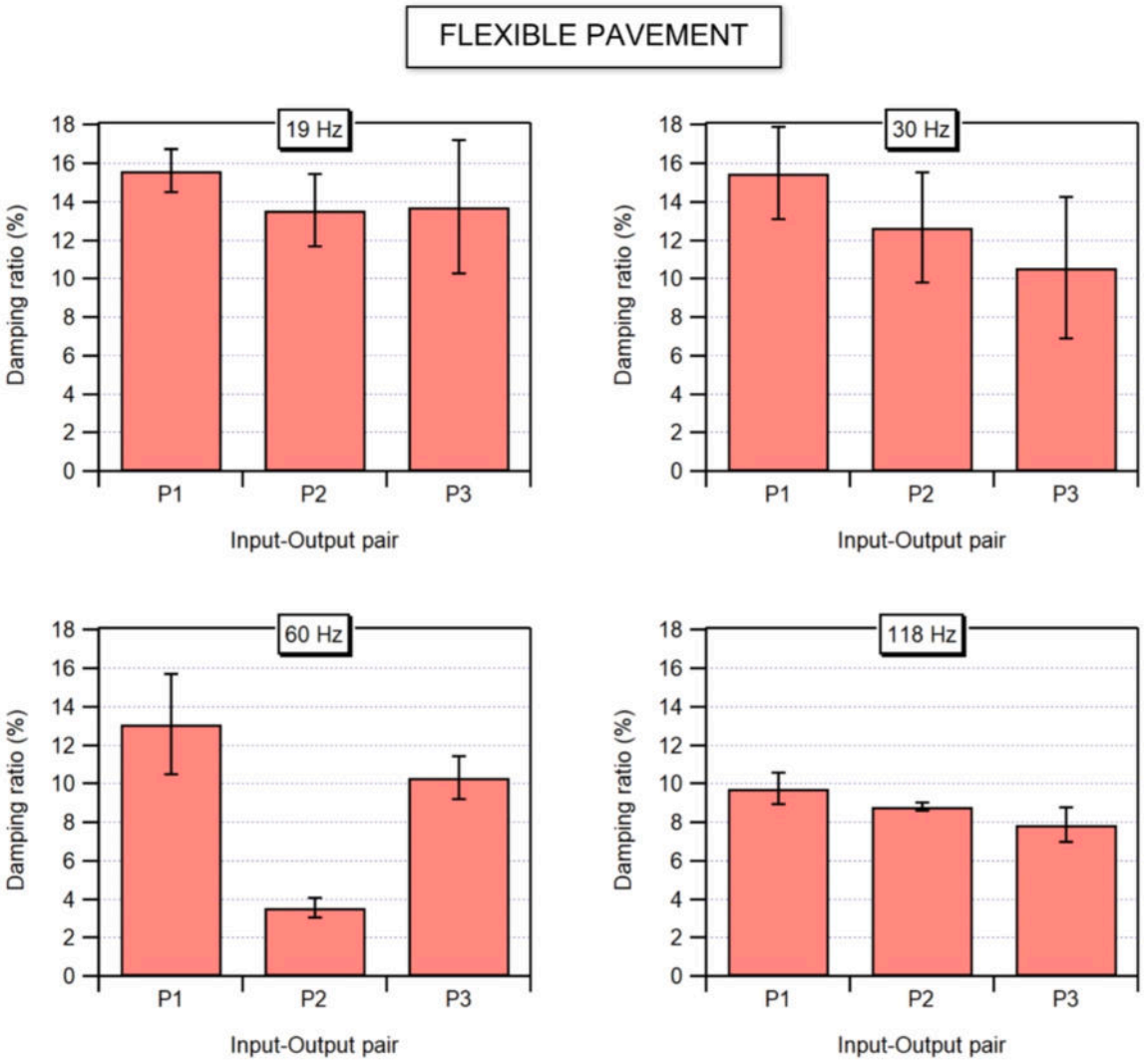

Fig. 6. Average damping ratios of the flexible pavement estimated using the DMPE-SD algorithm for the three examined input-output pairs. The error bars represent ± one standard deviation of the estimates over the range of model orders from 20 to 200.

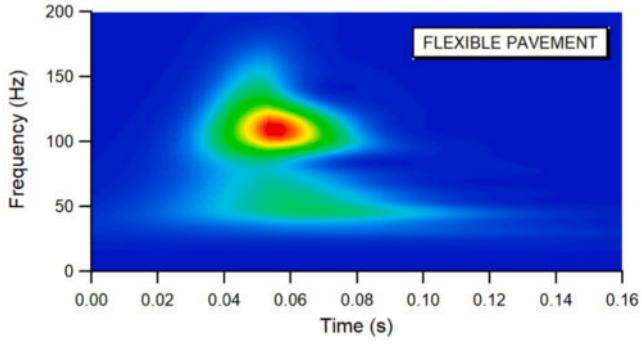

Fig. 7. Continuous wavelet transform of the response of the flexible pavement for the input-output pair P1.

authors propose to define a damping index based on the difference of acceleration values measured at different locations, but no values of measured damping properties are provided in the paper.

To the best of the authors' knowledge and based on the existing literature, no attempts have been made yet to exploit in-situ measurements to directly provide quantitative estimates of pavement damping properties across the range of frequencies that may be potentially excited by in-service loads. As mentioned earlier, assessing damping properties involves applying either continuous or impulse excitation to the examined system and analysing its vibration response using appropriate data interpretation techniques. Introducing continuous excitation to a real pavement system, however, would be impractical and expensive, since maintaining a stable and controlled excitation over large pavement sections would require specialised equipment that is bulky, difficult to deploy, and costly to implement in the field. In contrast, impact excitation provides a simpler, more cost-effective method for generating vibrations on pavement structures and has therefore been chosen in this study as a convenient and practical solution for in-situ damping measurement. From an operational point of view, the damping properties of the pavements were assessed by evaluating the attenuation, over time and at different frequencies, of the road surface vibrations experienced at a sensing point and caused by impact excitations at a different location. In particular, the damping ratio ξ, which is one of the most widely used parameters to characterise damping, was chosen as a quantitative and easily comparable measure of the frequency-dependent dissipative capacity of the pavements.

Two methodologies based on the analysis of data of the impulse response of the pavement system have been assessed for damping estimation at different vibration frequencies. The first one involves the use

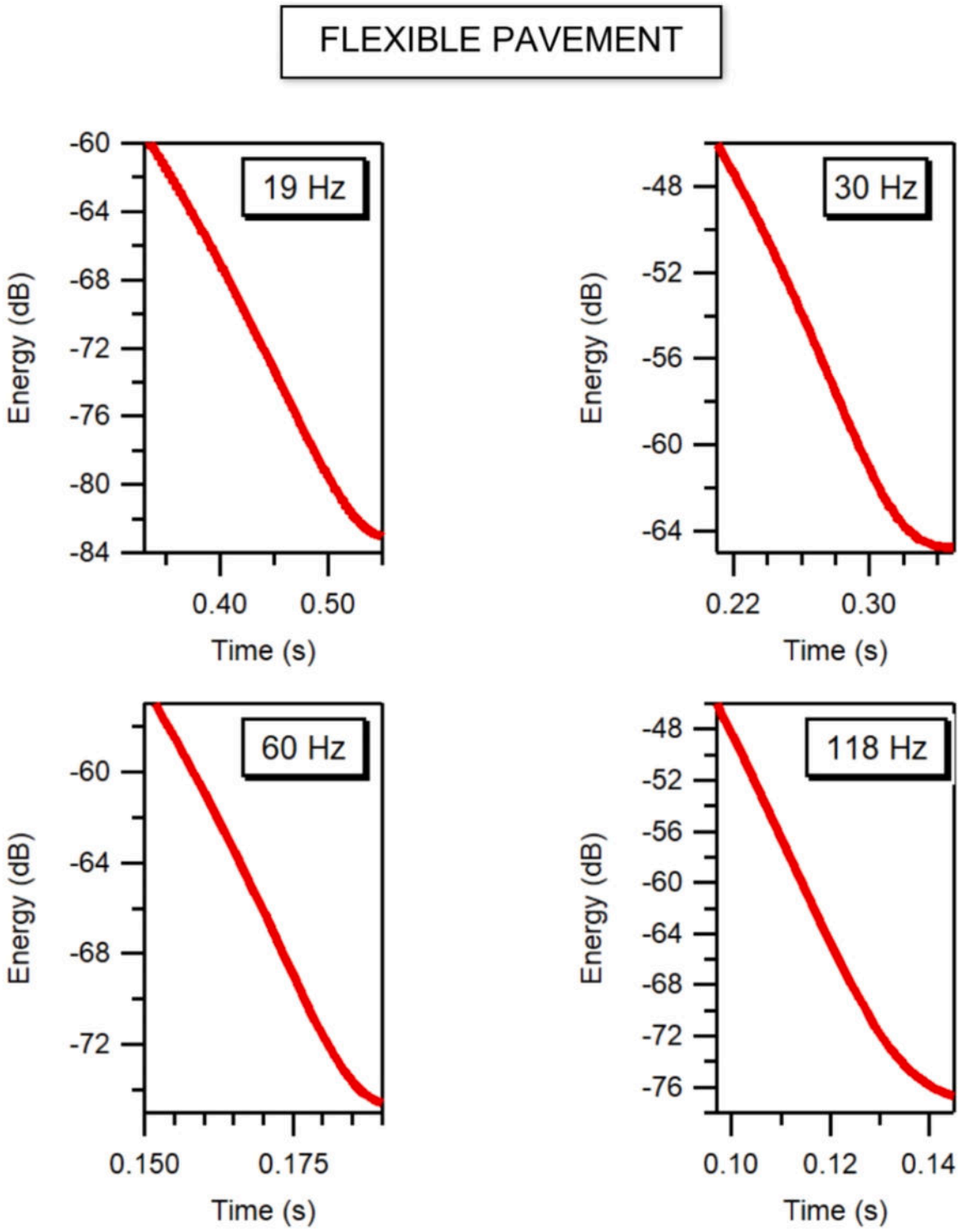

Fig. 8. Energy Decay curves extracted from the CWT map of Fig. 7 at the frequencies of 19, 30, 60, and 118 Hz.

of the Direct Modal Parameter Estimation (DMPE) algorithm in association with Stabilisation Diagrams (SDs) to evaluate the modal properties of physical vibration modes. It will be referred to as DMPE-SD procedure. The second one focuses on the application of time-frequency analysis for frequency decoupling and on the estimation of damping through the analysis of signal decay with time. Based on the use of Continuous Wavelet Transform (CWT) and the Energy Decay (ED) curve fitting, it will be called CWT-ED procedure. The two procedures were used on experimental data measured in situ from two pavement systems exhibiting significantly different structural and deformation behaviour to compare their effectiveness in identifying the damping properties of the examined structures.

2. Experimental approach and data analysis

2.1. Experimental tests

To assess the effectiveness and reliability of the two approaches

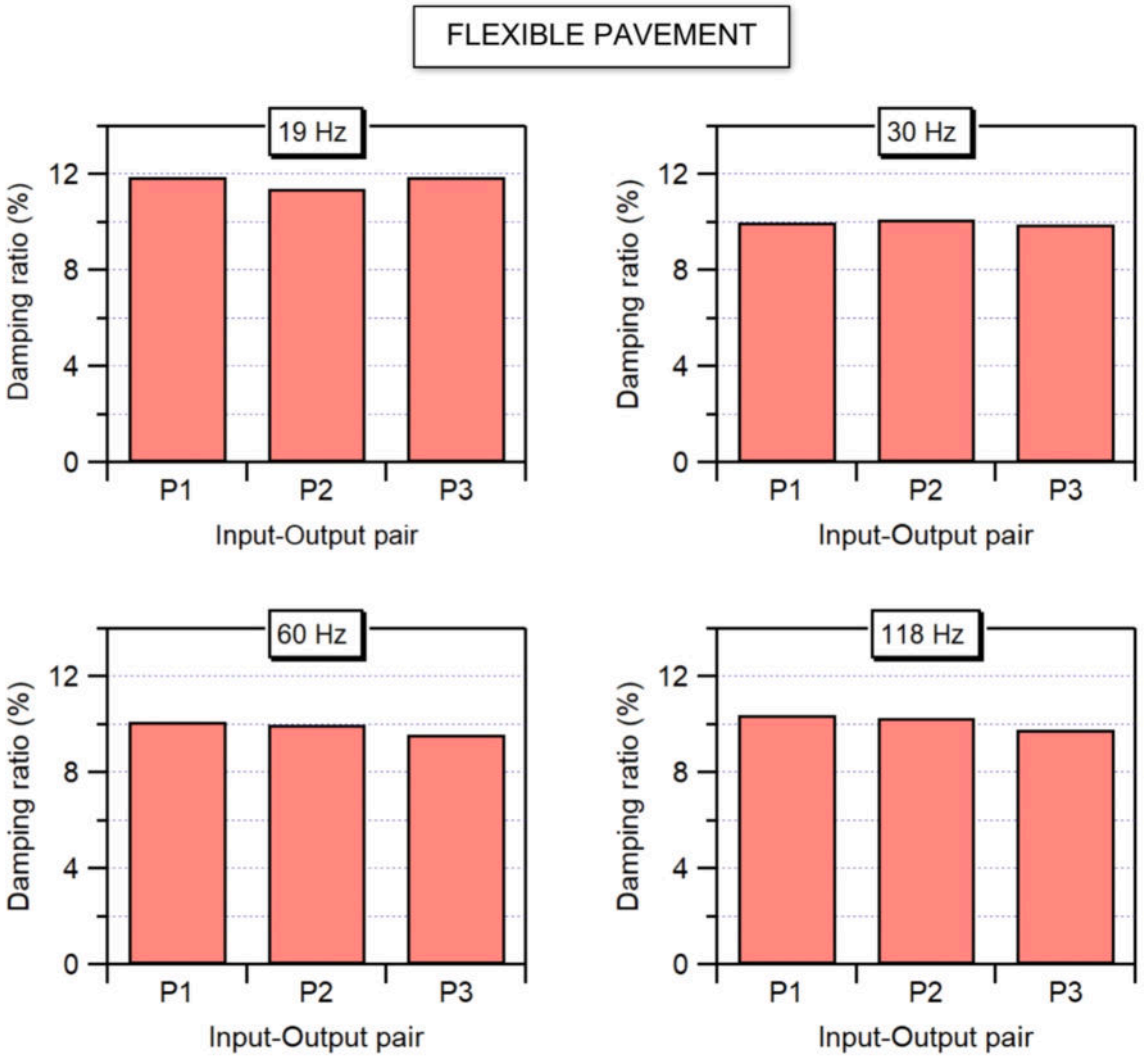

Fig. 9. Damping ratios of the flexible pavement estimated using the CWT-ED procedure for the three examined input-output pairs.

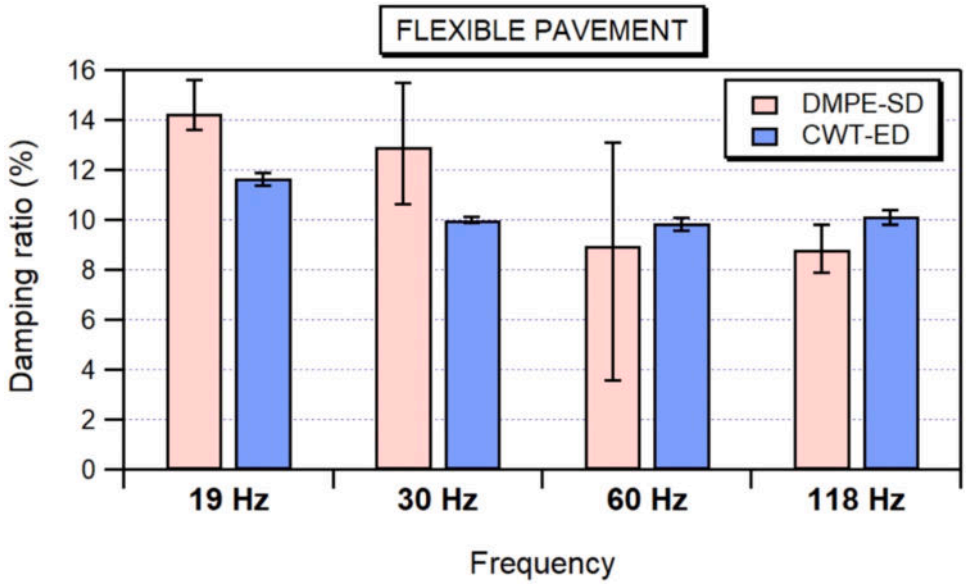

Fig. 10. Comparison of the damping ratios of the flexible pavement obtained from the DMPE-SD and CWT-ED procedures averaged over the three input-output pairs. The error bars indicate the range between the maximum and the minimum estimated values.

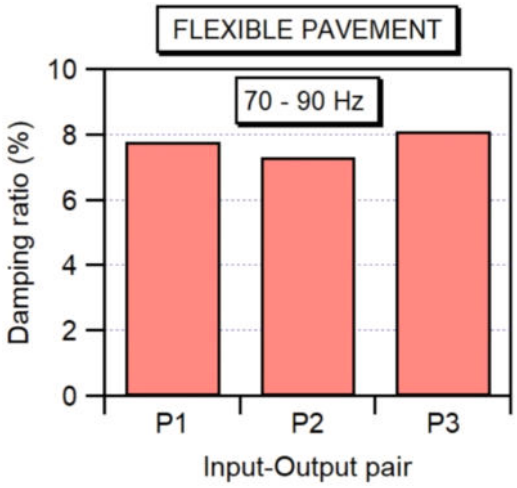

Fig. 11. Damping ratios evaluated across the frequency band 70–90 Hz using the CWD-ED.

considered for evaluating the dissipative properties of real pavement structures, in-situ tests were conducted on two different types of pavement structures: a flexible road pavement with an asphalt (bitumen-bound) surface layer and a rigid pavement composed of concrete slabs. In both cases, the pavements were subjected to impulsive loads applied using an impact hammer consisting of a 9 kg cylindrical steel mass equipped with a piezoelectric force transducer (HBM CFT+50 kN). During testing, a 3 mm thick neoprene pad was placed between the hammer tip and the rough pavement surface to ensure uniform load distribution over the impact region. Impacts with peak loads of about 40 kN were typically applied to induce vibrations in the system. The pavement response was measured using a Bruel & Kjaer 4370 piezo-ceramic accelerometer, which was attached to the pavement surface with a thin layer of butyl adhesive tape. The excitation and the response signals were fed into Bruel & Kjaer 2635 charge amplifiers and subsequently recorded with a National Instruments PC-controlled data acquisition unit at a sampling rate of 50 kSamples/s. Ten data sets were recorded for each measurement configuration to obtain the average frequency and impulse responses of the system. All tests were conducted at a temperature of 23°C ± 2°C, measured on the surface of the road pavement.

2.2. DMPE-SD procedure

The first procedure used for damping estimation is based on the use of an algorithm for identification of modal properties from the measured FRF of the examined system. The Direct Modal Parameter Estimation (DMPE) algorithm described in [30] was used to estimate the natural frequencies and the damping ratios of the vibration modes. It is well known that the choice of the model order used in modal identification analyses directly affects the accuracy and the relevance of the computed modal parameters [29]. A too low model order may prevent the algorithm from capturing the real vibration modes, whereas a too high model order can result in the algorithm detecting spurious (numerical) modes, associated with computational inaccuracies or noise in the data. Stabilisation Diagrams (SDs), where modal properties (such as natural frequency or damping ratio) are plotted as a function of the assumed model order, were therefore used to identify physical modes, which exhibit consistent frequency and damping values as the model order increases, in contrast to the irregular and discontinuous trends observed for spurious modes. The SDs were built using computed modes that satisfy criteria based on the simultaneous stability of frequency and damping ratio. Frequencies and damping ratios corresponding to models of increasing order were first computed, and the relative modes were plotted in the diagrams only if the differences in frequencies and damping ratios between consecutive model order iterations were below 1 % and 5 %, respectively. These threshold values are commonly recommended and widely used in the construction of stabilisation diagrams [29].

2.3. CWT-ED procedure

In the second procedure, the response of the pavement to the impact load was analysed using a Continuous Wavelet Transform (CWT), which performs a time-scale representation of the signal by decomposing it into wavelets that are scaled and translated versions of a chosen mother wavelet [29]. The scale can be correlated with frequency through a characteristic frequency of the wavelet, thus allowing for a time-frequency characterisation of the response. The wavelet analyses were carried out using complex-valued mother Morlet wavelet functions with 12 cycles, which provide excellent time-frequency localization

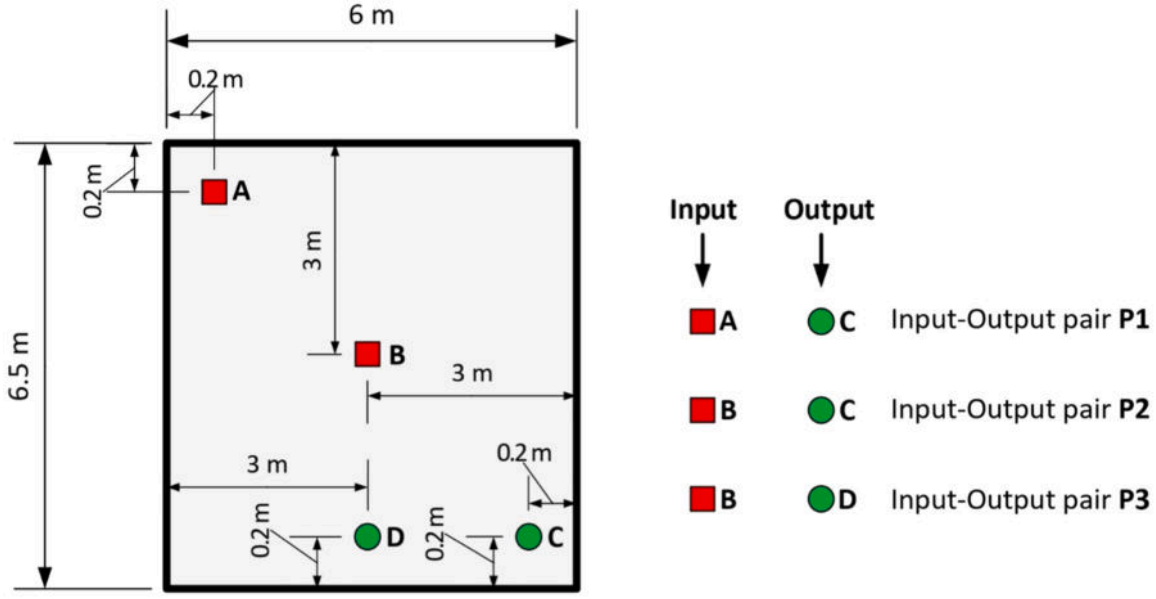

Fig. 12. Input-output pairs selected for the analysis of the slab of the rigid road pavement.

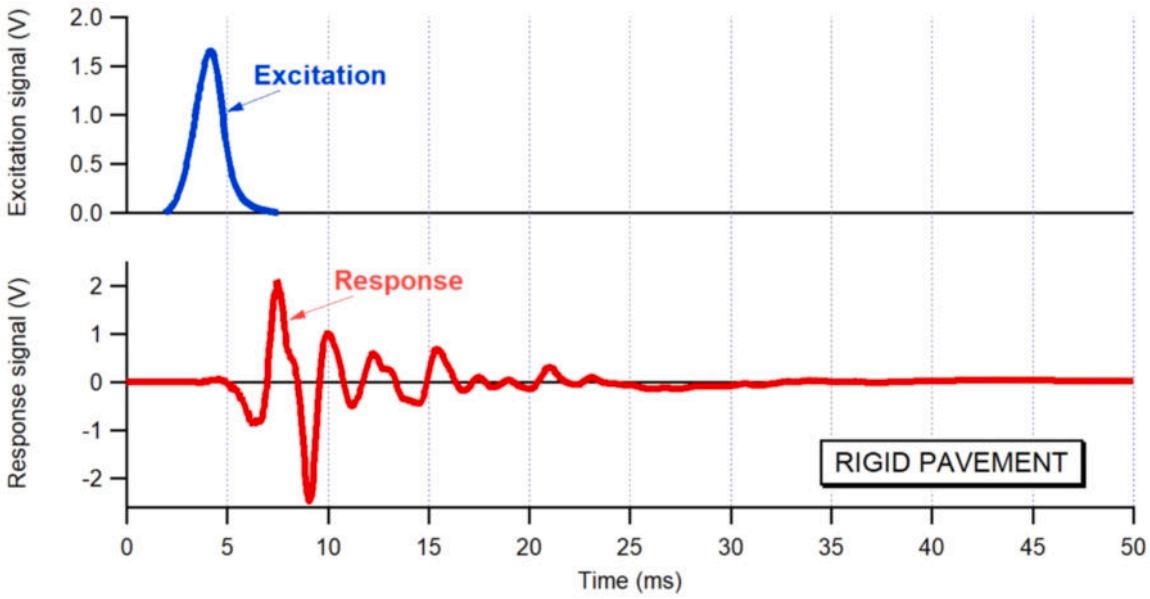

Fig. 13. Typical excitation and vibration signals acquired from measurements on the rigid pavement from the input-output pair P1.

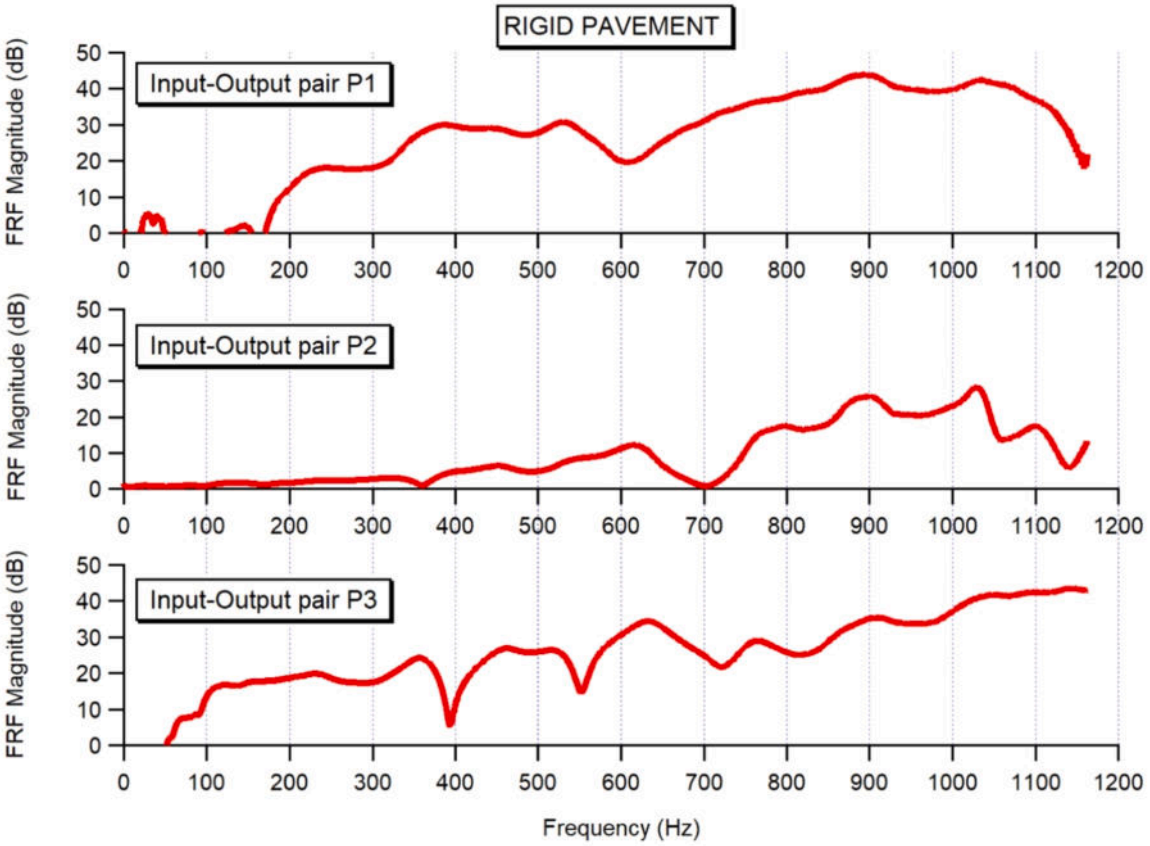

Fig. 14. FRFs of the rigid pavement acquired from the three examined input-output pairs.

properties [42,59]. The central frequency of the Morlet wavelet was used for scale-to-frequency mapping. The squared amplitudes extracted at the desired frequency from the wavelet transforms of the impact response were plotted in semi-logarithmic scale as a function of time. Care was taken to verify that the extracted signal was not in the region of the time-frequency plane (cone of influence) where, due to the finite length of the signal, edge effects become significant and wavelet results may become unreliable. To prevent these distortion effects, the acquisition duration was chosen to be long enough to move the edges of the acquired signal sufficiently away from the region of the impact response. In particular, an acquisition time of 8 s, with the pre-trigger set to position the impact response centrally within the full capture window, was adopted to ensure that the region of interest was outside the cone of influence, even at the lower frequencies examined in the analyses. The

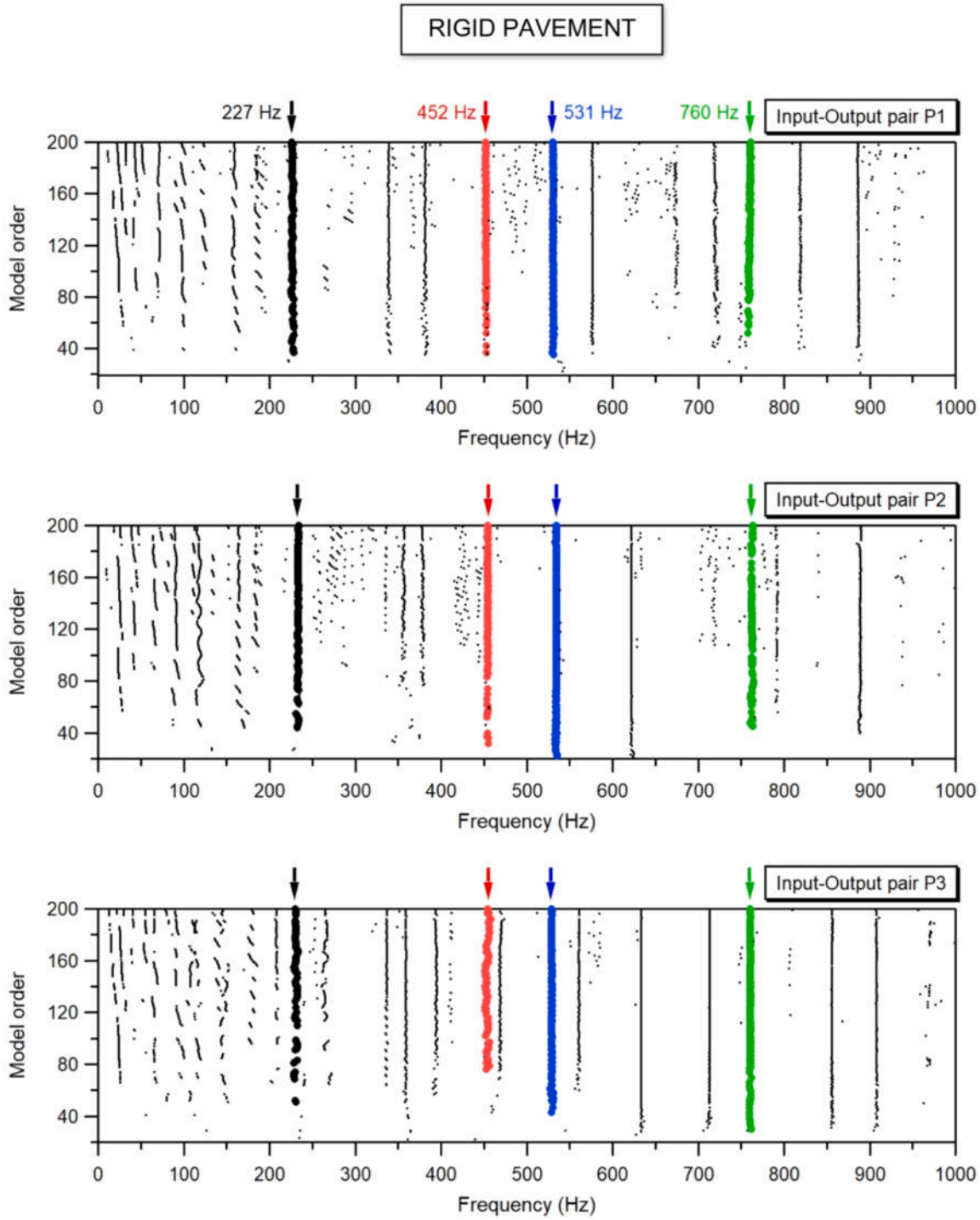

Fig. 15. Stabilisation diagrams of the modal response of the flexible pavement constructed using the DMPE algorithm for the three examined input-output pairs.

damping ratios of the pavement system were finally calculated from the slope of the straight line fitted to the energy decay (ED) curves [33]. Similarly to what was proposed in other investigations focusing on the decay of elastic or acoustic waves [60,61], a 15 dB range (between −2 dB and −17 dB from the maximum level) was chosen for the fitting. Preliminary analyses indicated that damping ratio values remained stable when considering intervals greater than 10 dB. Only linear regressions with correlation coefficients R^2 higher than 0.97 were considered for damping estimation.

3. Results and discussion

3.1. Flexible pavement

The damping behaviour of a flexible road pavement, consisting of an asphalt layer overlying a granular base, which rests on an underlying subgrade, was considered as a first test case. The asphalt layer includes a wearing surface (40 mm thick), an intermediate layer (60 mm thick), and a binder layer (80 mm thick). Flexible pavements are commonly used for low- to moderate-traffic roads and urban streets due to their lower construction and maintenance costs compared to rigid pavements.

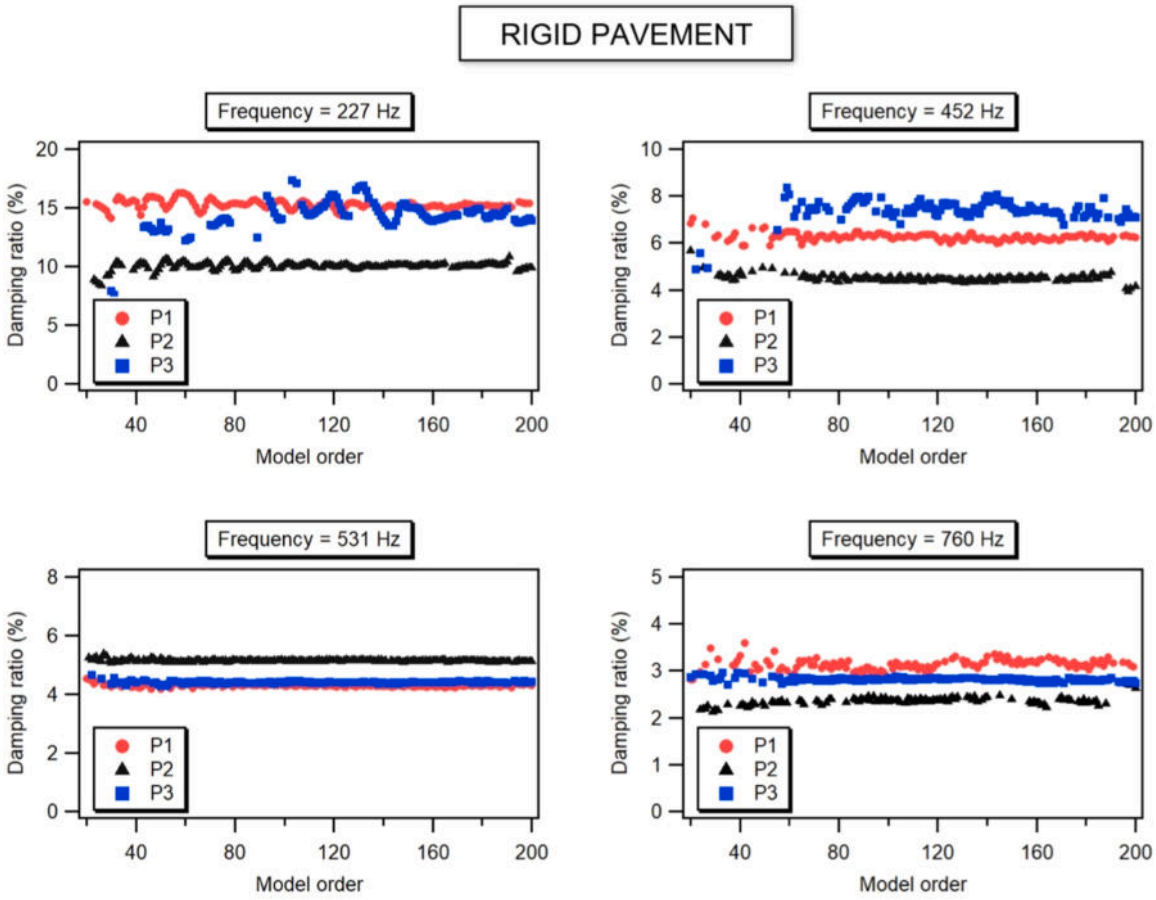

Fig. 16. Damping ratios of the rigid pavement estimated at 227 Hz, 452 Hz, 531 Hz, and 760 Hz using the DMPE-SD algorithm for the three examined input-output pairs.

Three different input-output (excitation-measurement) arrangements (P1, P2, and P3, as shown in Fig. 1) were chosen to explore how excitation and sensing locations affect the estimated damping values. Due to the inherent heterogeneity of the pavement structure -comprising various constituent phases of differing shapes, sizes, and properties (e.g., fillers, aggregates, additives, binders), along with irregularly distributed voids and defects- significant variability in the dissipative properties of the road pavement is expected at the local scale. Different and somewhat conflicting requirements were considered in the choice of the distance between the impact and measurement locations. The waves generated by the impact should be allowed to propagate for a length sufficient to both excite the multiple modes of the system and "average out" the effects of local irregularities or discontinuities, thus ensuring that the response measured at the sensing location is representative of the global dissipative behaviour of the pavement. In addition, close to the impact site, the response -and therefore the dissipative effects- may be dominated by the presence of local or high-frequency modes not especially relevant to the overall damping. Conversely, an excessive distance between the sensor and the impact site could attenuate the vibration signal to a level resulting in a low signal-to-noise ratio. Based on preliminary tests at different input-output distances, and in view of the characteristic geometric features of the examined pavements (with layer thicknesses on the order of several tens of cm), a distance of about 5 m between the impact excitation and the sensing location was considered to provide an appropriate balance between the various requirements.

Typical excitation and vibration signals are shown in Fig. 2 for the input-output pair P1, while Fig. 3 compares the FRFs for the three examined input-output arrangements. The response of the flexible road pavement is dominated by frequency components below 200 Hz and exhibits a spectral pattern lacking sharp, well-defined peaks, which suggests a dynamic behaviour governed by a combination of closely spaced or overlapping vibration modes that are extremely difficult to isolate and identify. We also observe that the FRFs obtained from the three measurement scenarios exhibit very similar spectral profiles, indicating that the choice of the input-output locations does not significantly affect the energy vs. frequency distribution of the impact response.

The DMPE-SD procedure was first assessed. The DMPE algorithm was applied to the FRFs of the pavement to estimate, for increasing model orders, the modal parameters for each of the different excitation and measurement locations. The computed modes meeting the chosen thresholds (differences between natural frequencies and damping ratios below 1 % and 5 %, respectively) are displayed as black dots or colour markers in the stabilisation diagram of Fig. 4, where the model order is plotted on the vertical axis as a function of frequency. Physical modes, which are expected to exhibit stable frequency values across different model orders, appear as sharp, straight vertical lines in the diagram. In contrast, spurious modes do not stabilise as the model order increases and appear discontinuous and irregularly scattered within the frequency–model order space. The diagrams in Fig. 4 show that many numerical modes extracted using the DMPE algorithm cannot be reliably associated with real vibration phenomena of the system, since they appear randomly dispersed and without clear and continuous vertical alignment. On the other hand, various computed modes appear with good consistency at stable frequencies and can, with reasonable confidence, be assumed as physical modes of vibration of the pavement. Despite the similar spectral profiles of the FRFs measured for the three measurement arrangements, some modes that are recognised as physical

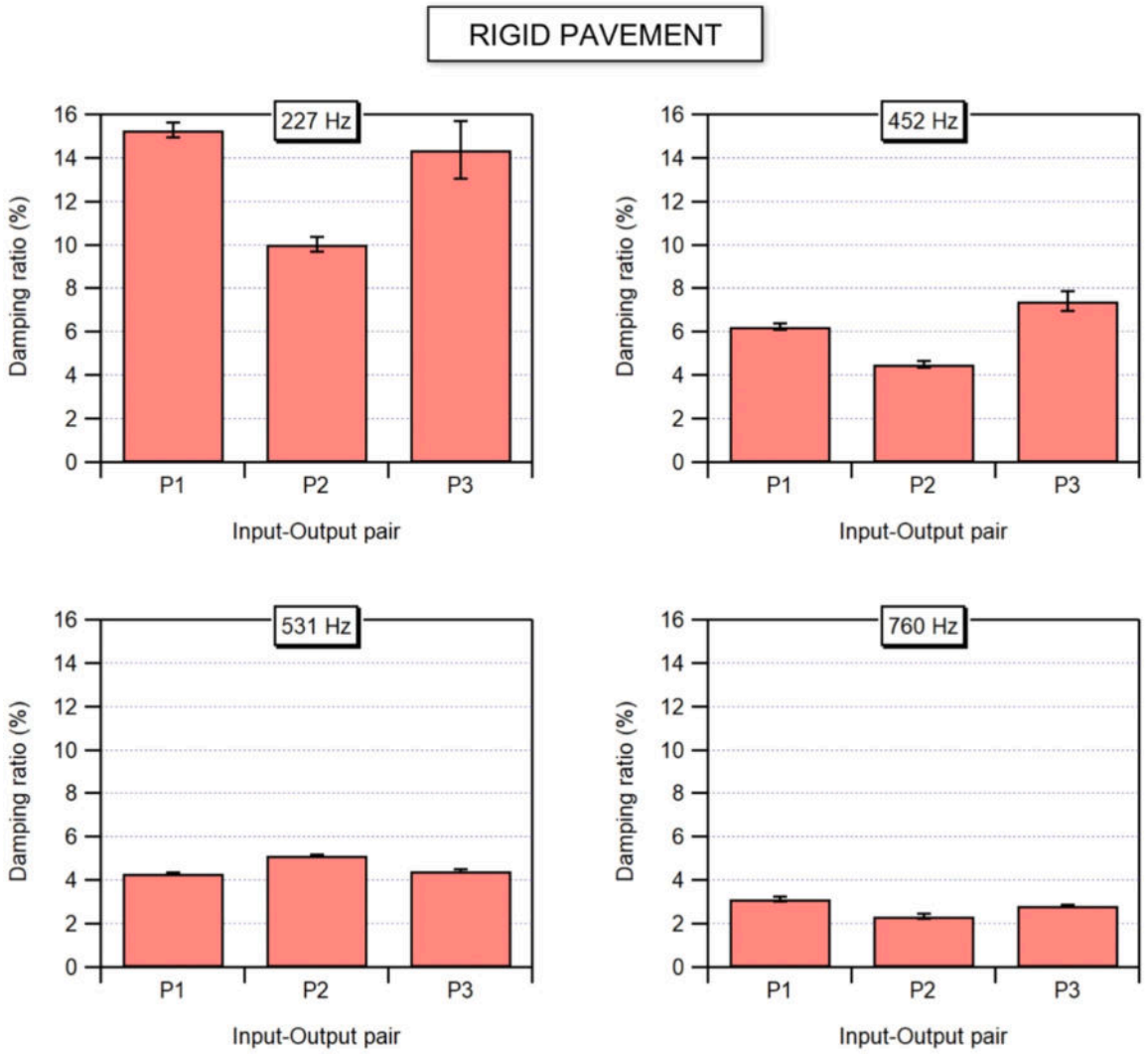

Fig. 17. Average damping ratios of the rigid pavement estimated using the DMPE-SD algorithm for the three examined input-output pairs. The error bars represent ± one standard deviation of the estimates over the range of model orders from 20 to 200.

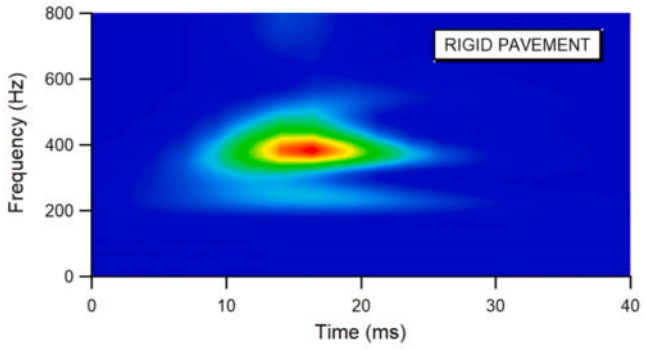

Fig. 18. Continuous wavelet transform of the response of the rigid pavement for the input-output pair P1.

in the SD for one input-output pair are not visible in the SD of a different input-output pair. For instance, the mode at about 69 Hz may be clearly detected in the SD for the P2 testing arrangement, but the same mode does not appear in the SDs for the P1 and P3 input/output pairs.

Four physical modes detected in all three testing configurations (corresponding to the nominal frequencies of about 19 Hz, 30 Hz, 60 Hz and 118 Hz and plotted with thick colour markers in the SDs of Fig. 4) were selected to evaluate the performance of the approach based on modal parameter identification for characterising the damping properties of the pavement. The damping ratios estimated by the DMPE algorithm for these four frequencies are plotted as a function of the model order in the diagrams of Fig. 5. It should be noted that, to account for noise effects and numerical inaccuracies, all computed modes with frequencies within a 1 Hz range of the four selected frequencies were included in the analysis. We see that for the highest frequency (118 Hz) the damping ratios tend to stabilise and converge to practically the same value for all three input-output pairs. For the lower modal frequencies, however, the DMPE computations yield damping values that not only exhibit a very large scatter across model orders but may also vary significantly depending on the input-output pair considered. The large fluctuations of the damping ratios calculated for the lower frequency modes may be related to the relatively low amplitude of these modes, which results in reduced contributions, with respect to the 118 Hz mode, to the DMPE process, thus leading to inaccuracies and bias in the damping evaluation. As a possible approach for addressing this scatter and obtaining a more representative estimate of the damping ratio, the damping values generated by the DMPE algorithm for different model orders were averaged over the modal order range from 20 to 200. The average damping ratios obtained from the analysis of data from the three

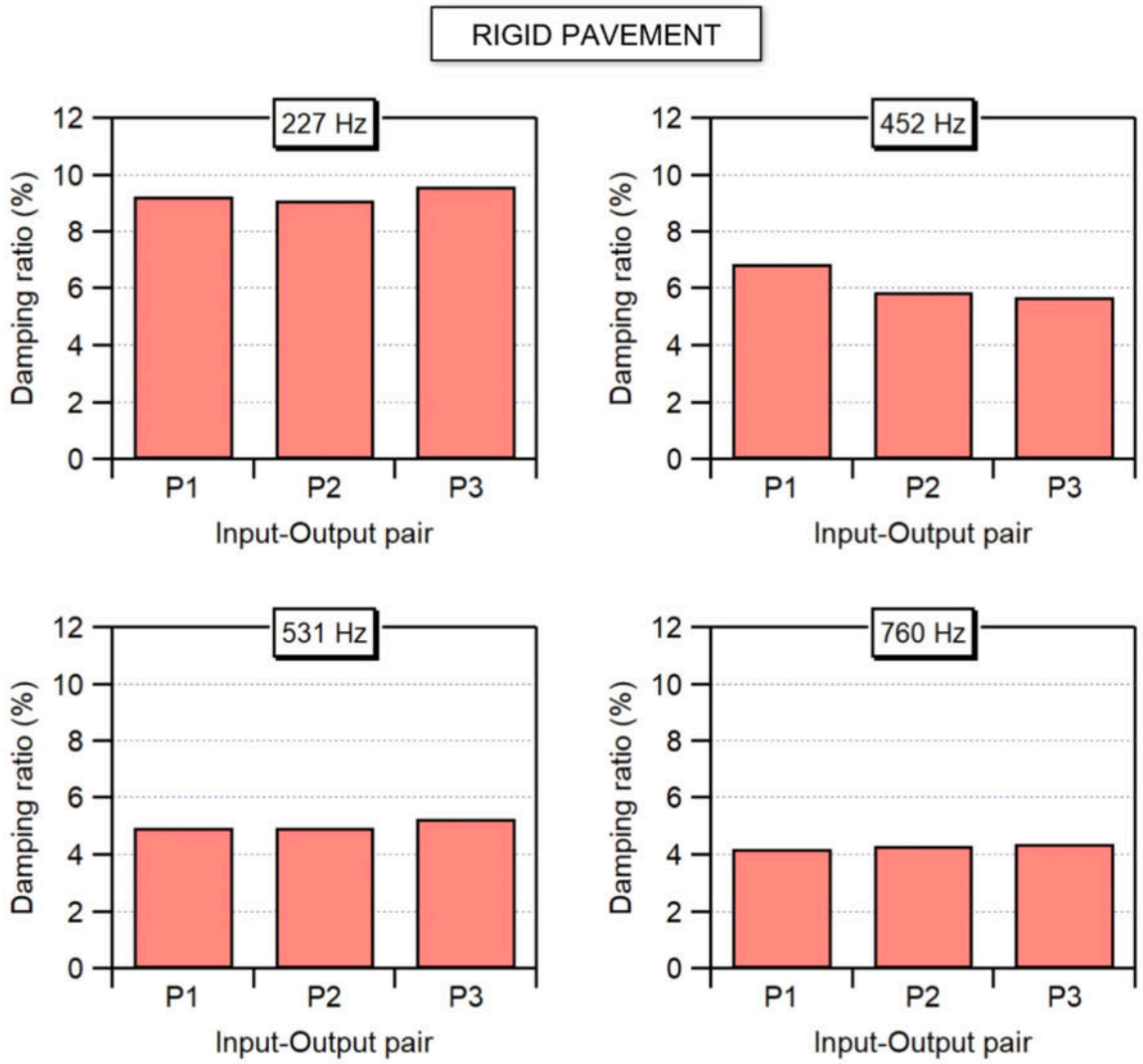

Fig. 19. Damping ratios of the rigid pavement estimated using the CWT-ED procedure for the three examined input-output pairs.

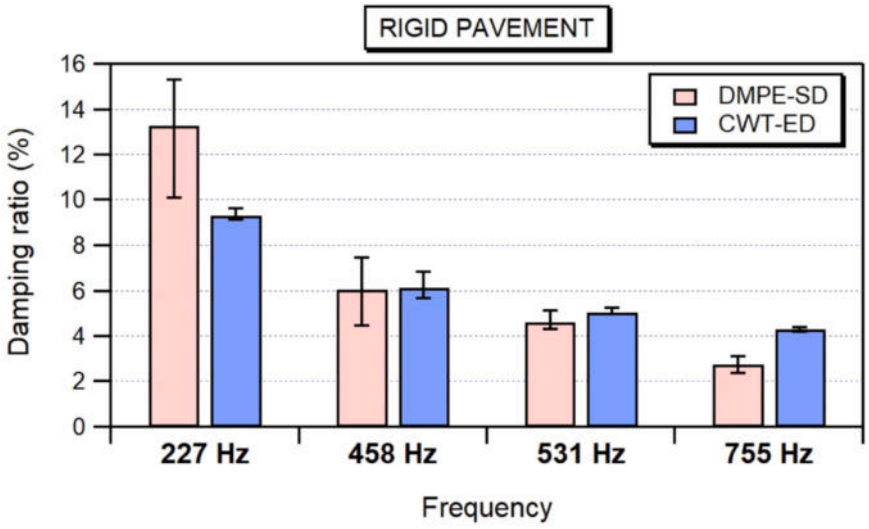

Fig. 20. Comparison of the damping ratios of the rigid pavement obtained from the DMPE-SD and CWT-ED procedures averaged over the three input-output pairs. The error bars indicate the range between the maximum and the minimum estimated values.

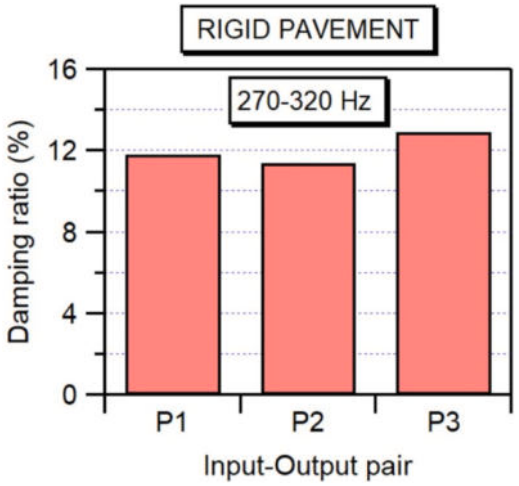

Fig. 21. Damping ratios evaluated across the frequency band 270–320 Hz using the CWD-ED.

input-output scenarios are compared in the graphs of Fig. 6. The error bars shown in these graphs highlight the significant degree of dispersion, particularly for lower frequencies, in the damping ratios computed across the range of model orders examined. The data in Fig. 6 also show that substantially different damping properties may be obtained using the DMPE-SD procedure when analysing measurements from various excitation and sensing locations.

To address these issues, the alternative CWT-ED procedure based on continuous wavelet analysis was applied to estimate the damping ratios of the flexible road pavement over the range of investigated frequencies. The response to impact of the pavement was transformed to the time-frequency domain using the CWT, which enables the decoupling of the response into time signals at different frequencies. As an example, a typical wavelet transform of the impact response obtained from measurement acquired for the input-output pair P1 is shown in Fig. 7, while energy decay curves extracted as cross-sections at different frequencies from the CWT map are displayed in the graphs of Fig. 8. The damping ratios for the three input-output pairs, calculated as the slope of the line that best fits the decay curves over a 15 dB range, are shown in Fig. 9 for the same frequencies previously examined using the DMPE-SD procedure. We see that the damping ratios estimated using the CWT-ED approach are nearly independent of the chosen input-output pairing scheme, unlike those obtained via the DMPE-SD procedure, which yield highly variable results depending on the input-output arrangement considered (see Fig. 6). This indicates a low sensitivity of the wavelet-based decay rate method to changes in the excitation and sensing location, highlighting its superior robustness in estimating pavement damping properties. A direct comparison of the damping ratios calculated using the two procedures and averaged over the three input-output measurement configurations is presented in Fig. 10. Comparable results between DMPE-SD and CWT-ED estimates are found for the higher frequency modes (118 Hz), while a significant difference is observed for the lower frequency modes (19, 30 and 60 Hz). The greater scatter in the damping ratios calculated via the DMPE-SD procedure is also evident when comparing the ranges between the maximum and minimum estimates provided by the two approaches across the three input-output pairs.

It might be worth noting that, besides its higher reliability, the CWT-ED approach provides additional benefits compared to the DMPE-SD approach. Firstly, the CWT-ED approach is particularly advantageous because it can identify damping properties from output-only measurements, making it a practical choice when input measurements are unavailable or restricted. A further advantage of the CWT-ED approach is that prior knowledge of natural frequencies is not required for its application. This characteristic is particularly beneficial when analysing systems with high modal density, as the examined pavement system, where identifying natural frequencies is difficult or even infeasible due to closely spaced and low-amplitude vibration modes. In such cases, band-averaged damping ratios can be computed from the energy decay curves obtained by integrating the wavelet transform data over the frequency band of interest. As an example, the graphs in Fig. 11 show the damping ratios evaluated across the frequency band 70–90 Hz, where no clear physical frequencies can be identified through the stabilisation diagrams for the considered input-output pairs. Within this frequency range, the CWT-ED method still provides damping ratios that are nearly independent of the chosen input-output locations, confirming the broader applicability and greater effectiveness of the wavelet-decay rate approach compared to the procedure that relies on direct modal parameter identification.

3.2. *Rigid pavement*

A second series of experimental tests was conducted on a rigid pavement composed of Portland cement concrete slabs (5.20 m by 5 m in size and 0.3 m thick), reinforced with a steel mesh and resting on a granular subgrade. The concrete slabs are separated by flexible joints to accommodate thermal or moisture-induced expansion and contraction. This type of pavement, whose structural and dynamic properties are significantly different from those of the flexible pavement examined in the previous section, is typically employed in high-traffic roads and airport runways due to its high load-bearing capacity, durability, and resistance to environmental factors.

Three different input-output arrangements were again chosen to assess the sensitivity of damping estimations to the excitation and sensing locations (Fig. 12). Since preliminary tests indicated that the slabs largely act as independent units when responding to external excitation loads, the impact and measurement points were chosen on the same slab.

Figs. 13 and 14 show typical acquired signals and the FRFs obtained for the three testing configurations, respectively. It can be noticed that the spectral response reveals strongly coupled modes regardless of the input-output pair considered, leading to considerable difficulty in distinguishing closely spaced natural frequencies. Due to the high structural stiffness of concrete slabs, the dynamic response of the rigid pavement exhibits a predominance of higher frequency components compared to the flexible pavement. A maximum frequency of 1200 Hz was considered for the subsequent analysis, as dynamic loads with frequencies of up to hundreds of Hz can, for example, be generated by vehicles during acceleration or deceleration [62]. It is also evident that the spectral distribution of the impact response of the rigid slab is influenced by the excitation and sensing positions to a much greater extent than in the flexible pavement. This was expected due to the limited size of the slab structure and the stronger influence of boundary effects compared with the primarily one-dimensional geometry of the road pavement as examined in the previous section.

Again, the DMPE-SD procedure was first applied. The stabilisation diagrams describing the dynamic behaviour of the rigid pavement for the three different testing configurations are shown in Fig. 15. Similarly to what was observed for the flexible pavement system, and due to the very high modal density, only a relatively small number of physical modes can be confidently identified from the stabilisation diagrams, while many DMPE-computed modes exhibit discontinuous or erratic trends in terms of frequency and damping ratio as the model order increases.

As done for the flexible pavement case, four natural frequencies associated with physical vibration modes visible in all three input-output scenarios (227 Hz, 452 Hz, 531 Hz, and 760 Hz), were selected to compare the effectiveness of the examined methods for characterising the damping properties of the rigid pavement. The damping ratios computed by the DMPE algorithm are reported as a function of model

order in the graphs of Fig. 16. For the lower modal frequencies (227 and 452 Hz), the damping ratios display high scatter across different model orders, but this dispersion tends to lessen with increasing order values. The estimates of the damping ratio, however, are significantly affected by the choice of the input-output locations. In contrast, the damping ratios are almost constant and not greatly affected by the excitation and measurement locations for the highest frequencies (531 Hz and 760 Hz). The average damping ratios estimated by the DMPE-SD over the three input-output locations are summarized in the graphs of Fig. 17. The trends exhibited by the graphs of Figs. 16 and 17 appear consistent with those observed in the flexible pavement case, with computed vibration modes of low amplitude or characterised by poorer frequency stability (likely due to the presence of narrowly spaced modes) generally associated with damping estimates showing higher variability with model order and a strong dependence on the chosen input-output locations.

The data acquired on the rigid pavement were then processed using the CWT-ED procedure, by analysing the decay with time of cross-sections extracted from CWT maps such as that shown in Fig. 18 for the input-output pair P1. As opposed to the DMPE-SD procedure, the CWT-ED approach generates estimates of damping ratios that are, for all four examined frequencies, only slightly influenced by the choice of the points used for impact and vibration measurement (Fig. 19). The data reported in the graph of Fig. 20, which compare the average damping ratios obtained by the DMPE-SD and the CWT-ED procedures, show the significant difference in both mean value and dispersion provided by the two approaches at the lower frequencies; these results confirm the higher reliability and robustness of the CWT-ED approach for characterisation of damping in road pavements in comparison to the DMPE-SD procedure.

As a final example, the plots in Fig. 21 show the damping ratios computed for the three input-output scenarios by applying the CWT-EDC approach after averaging the wavelet transform data over the frequency range 270–320 Hz. While no physical frequencies can be reliably identified (and therefore no damping ratios can be estimated) in this range using the modal parameter identification technique (see the stabilisation diagrams of Fig. 15), the wavelet analysis provides values of damping ratios that are reasonably close to each other for the different input-output locations, further confirming the effectiveness of the CWT-ED approach for the assessment of the damping properties of road pavements.

4. Conclusions

Although the dissipative properties of road pavements play a key role in mitigating the adverse effects of vibrations on humans and structures, the field assessment of road pavement damping remains an open issue. To contribute to this matter, the paper compares two experimental in-situ procedures for evaluating the damping properties of road pavements over a range of frequencies representative of service loading conditions. The first procedure (DMPE-SD) involves the use of a modal parameter identification algorithm in conjunction with a stabilisation diagram tool. The second procedure (CWT-ED) exploits the continuous wavelet transform to obtain a time-frequency characterisation of the response and calculates the damping ratio from the decay curve extracted from the transform. Experimental campaigns were carried out on a flexible (asphalt-based) pavement and a rigid (concrete) pavement, which exhibit significantly different stiffness properties and spectral responses. An instrumented hammer and an accelerometer were used respectively to apply an impulsive load and to acquire the pavement's response. Three different input-output locations and four physical frequencies were chosen to assess and compare effectiveness, reliability and robustness of the two approaches.

The main findings of the study are summarized below.

- The dynamic response to impact excitation of both flexible and rigid pavements exhibits a high modal density, with multiple closely spaced vibration modes. The spectral profile of the response of the rigid pavement shows a higher frequency content and a much greater dependence on the chosen input-output pairs than the flexible pavement.

- The damping ratios estimated by the DMPE algorithm generally exhibit large fluctuations, especially at frequencies associated with low-amplitude vibration modes, depending on the model order assumed in the calculations. To account for this scatter, the damping ratios computed by the DMPE algorithm and identified as stable by the SD tool were averaged over the examined range of modal orders to obtain the damping ratios identified by the DMPE-SD procedure for the examined frequency. The values of the damping ratios estimated through this approach often show, however, a very large dependence on the input-output pair chosen for the tests.

- In contrast to the DMPE-SD-based approach, the CWT-ED procedure was found to provide values of damping ratios that are only slightly affected by the choice of the input-output locations for all examined frequencies in both rigid and flexible pavements, indicating a higher robustness for the in-situ identification of damping properties In addition, the CWT-ED approach does not necessitate prior knowledge of modal frequencies and is based on output-only data, thus offering significant potential for easy implementation as a field technique for the characterisation of dissipative properties in road pavements with different configurations or designs and across a wide spectrum of excitation conditions.

- Further analyses are required to quantitatively evaluate the accuracy of the CWT-ED technique and to explore its application for a direct in-situ assessment of the overall dissipative performance potentially achievable using enhanced layers (i.e., nano- or graphene-modified asphalts or concrete, high porosity and rubberized layers, engineered composites, etc.) or by the optimisation of the pavement configuration. Additional research work could be directed towards examining the technique as a possible tool for monitoring the health of road pavements using changes in damping as a means of detecting structural damage.

CRediT authorship contribution statement

G. Loi: Conceptualization, Methodology, Investigation, Formal analysis, Writing - original draft, Writing - review & editing. **M.C. Porcu:** Conceptualization, Methodology, Investigation, Formal analysis, Writing - original draft, Writing - review & editing. **F. Maltinti:** Conceptualization, Writing – review & editing, Writing – original draft, Data curation, Conceptualization. **M. Coni:** Funding acquisition, Project administration, Writing - review & editing. **F. Aymerich:** Conceptualization, Methodology, Investigation, Formal analysis, Writing - original draft, Writing - review & editing.

Declaration of Competing Interest

The authors declare that they have no known competing financial interests or personal relationships that could have appeared to influence the work reported in this paper: As declared in the acknowledge, this study was financially supported by the Sardinia Regional Government through the project titled "*Research and Study for Innovative Monitoring of Road Infrastructures and for the Safety of Bridges and Viaducts*", 2020–2024 (RAS No. 67/28 – L.R. No. 8/2018).

Acknowledgements

This study was financially supported by the Sardinia Regional Government through the project titled "Research and Study for Innovative Monitoring of Road Infrastructures and for the Safety of Bridges and Viaducts", 2020–2024 (RAS No. 67/28 – L.R. No. 8/2018).

Data Availability

Data will be made available on request.

References

[1] Environmental Noise Guidelines for the European Region; World Health Organization, Regional Office for Europe: Copenhagen, Denmark, 2018; ISBN 978-92-890-5356-3.

[2] M. Ohiduzzaman, O. Sirin, E. Kassem, J. Rochat, State-of-the-art review on sustainable design and construction of quieter pavements—part 1: traffic noise measurement and abatement techniques, Sustainability 8 (2016) 742, https://doi.org/10.3390/su8080742.

[3] J.C. Castellanos, F. Fruett, Embedded system to evaluate the passenger comfort in public transportation based on dynamical vehicle behavior with user's feedback, Measurement 47 (2014) 442–451, https://doi.org/10.1016/j.measurement.2013.08.068.

[4] M. Coni, F. Maltinti, F. Pinna, N. Rassu, C. Garau, B. Barabino, G. Maternini, On-board comfort of different age passengers and bus-lane characteristics (Lecture Notes in Computer Science), in: O. Gervasi, B. Murgante, S. Misra, C. Garau, I. Blečić, D. Taniar, B.O. Apduhan, A.M.A.C. Rocha, E. Tarantino, C.M. Torre, Y. Karaca (Eds.), Computational Science and Its Applications – ICCSA 2020, 12255, Springer International Publishing: Cham, 2020, pp. 658–672 (Lecture Notes in Computer Science).

[5] S. Schubert, D. Gsell, R. Steiger, G. Feltrin, Influence of asphalt pavement on damping ratio and resonance frequencies of timber bridges, Eng. Struct. 32 (2010) 3122–3129, https://doi.org/10.1016/j.engstruct.2010.05.031.

[6] B. Weber, Dynamic properties of footbridges: influence of asphalt pavement and support conditions, MATEC Web Conf. 24 (2015) 01004, https://doi.org/10.1051/matecconf/20152401004.

[7] J. Ren, Y. Chen, Z. Sun, Y. Zhang, A vehicle-bridge interaction vibration model considering bridge deck pavement, J. Low. Freq. Noise Vib. Act. Control 42 (2023) 146–172, https://doi.org/10.1177/14613484221122736.

[8] R.D. Quinteros, A. Barbat, L.G. Nallim, S. Oller, Numerical study of vibrations induced by traffic in structures and a screen alternative for its mitigation, Int. J. Archit. Herit. 15 (2021) 1512–1525, https://doi.org/10.1080/15583058.2019.1706790.

[9] P. Clemente, D. Rinaldis, Protection of a monumental building against traffic-induced vibrations, Soil Dyn. Earthq. Eng. 17 (1998) 289–296, https://doi.org/10.1016/S0267-7261(98)00012-8.

[10] A. Pau, F. Vestroni, Vibration assessment and structural monitoring of the basilica of maxentius in Rome, Mech. Syst. Signal Process. 41 (2013) 454–466, https://doi.org/10.1016/j.ymssp.2013.05.009.

[11] J. Huang, M. Losa, P. Leandri, S.G. Kumar, J. Zhang, Y. Sun, Potential anti-vibration pavements with damping layer: finite element (FE) modeling, validation, and parametrical studies, Constr. Build. Mater. 281 (2021) 122550, https://doi.org/10.1016/j.conbuildmat.2021.122550.

[12] R.N. Modi, Causes of increasing vehicle maintenance cost and pavement condition at chhapi railway crossing, Int. J. Transp. Eng. Traffic Syst. 3 (2017) 20–25.

[13] K. Lou, P. Xiao, A. Kang, Z. Wu, X. Dong, Effects of asphalt pavement characteristics on traffic noise reduction in different frequencies, Transp. Res. Part D Transp. Environ. 106 (2022) 103259, https://doi.org/10.1016/j.trd.2022.103259.

[14] S. Ling, F. Yu, D. Sun, G. Sun, L. Xu, A comprehensive review of tire-pavement noise: generation mechanism, measurement methods, and quiet asphalt pavement, J. Clean. Prod. 287 (2021) 125056, https://doi.org/10.1016/j.jclepro.2020.125056.

[15] K.P. Biligiri, K. Kaloush, J. Uzan, Evaluation of asphalt mixtures' viscoelastic properties using phase angle relationships, Int. J. Pavement Eng. 11 (2010) 143–152, https://doi.org/10.1080/10298430903033354.

[16] J. Huang, P. Leandri, G. Cuciniello, M. Losa, Mix design and laboratory characterisation of rubberised mixture used as damping layer in pavements, Int. J. Pavement Eng. 23 (2022) 2746–2760, https://doi.org/10.1080/10298436.2020.1869975.

[17] E. Quan, H. Xu, Z. Sun, Composition optimization and damping performance evaluation of porous asphalt mixture containing recycled crumb rubber, Sustainability 14 (2022) 2696, https://doi.org/10.3390/su14052696.

[18] P. Sadeghi, A. Karimi, S. Torbatifard, A. Goli, A comprehensive evaluation of damping, vibration, and dynamic modulus in reclaimed asphalt pavement: the role of rejuvenators, polymer, temperature, and aging, Case Stud. Constr. Mater. 21 (2024) e03366, https://doi.org/10.1016/j.cscm.2024.e03366.

[19] C.-M. Kuo, C.-C. Lin, C.-H. Huang, Y.-C. Lai, Issues in simulating falling weight deflectometer test on concrete pavements, KSCE J. Civ. Eng. 20 (2016) 702–708, https://doi.org/10.1007/s12205-015-0299-y.

[20] W. Uddin, S. Garza, 3D-FE simulation study of structural response analysis for pavement-subgrade systems subjected to dynamic loads. Proceedings of the Pavements and Materials, American Society of Civil Engineers: Los Angeles, California, United States, 2010, pp. 170–181.

[21] G. Bazi, J. Gagnon, Effects of FWD deflection time history parameters on dynamic backcalculation. Proceedings of the Airfield and Highway Pavements 2023, American Society of Civil Engineers: Austin, Texas, 2023, pp. 340–352.

[22] G. Fu, D. Cao, G.P. Ong, J. Wang, D. Sha, A viscoelastic wave propagation approach for dynamic backcalculation of layer properties of asphalt pavements under an impact load, Comput. Geotech. 176 (2024) 106752, https://doi.org/10.1016/j.compgeo.2024.106752.

[23] Chopra AK Dynamics of Structures. Theory and Application to Earthquake Engineering; Prentice Hall, 2000;

[24] J. Huang, X. Li, J. Zhang, Y. Sun, J. Ren, Determining the Rayleigh Damping Parameters of Flexible Pavements for Finite Element Modeling, J. Vib. Control 28 (2022) 3181–3194, https://doi.org/10.1177/10775463211026763.

[25] I.L. Al-Qadi, H. Wang, P.J. Yoo, S.H. Dessouky, Dynamic analysis and in situ validation of perpetual pavement response to vehicular loading, Transp. Res. Rec. 2087 (2008) 29–39, https://doi.org/10.3141/2087-04.

[26] M.S. Cao, G.G. Sha, Y.F. Gao, W. Ostachowicz, Structural damage identification using damping: a compendium of uses and features, Smart Mater. Struct. 26 (2017) 043001, https://doi.org/10.1088/1361-665X/aa550a.

[27] A.K. Zrayka, E. Mucchi, A comparison among modal parameter extraction methods, SN Appl. Sci. 1 (2019) 781, https://doi.org/10.1007/s42452-019-0806-8.

[28] J. He, Z.F. Fu, Modal analysis, Butterworth-Heinemann, Oxford, 2001.

[29] P. Avitabile, Modal testing. A Practitioner's Guide, John Wiley & Sons Ltd, Chichester, 2018.

[30] B. Chomette, A. Mamou-Mani, Modal control based on direct modal parameters estimation, J. Vib. Control 24 (2018) 2389–2399, https://doi.org/10.1177/1077546317726615.

[31] H.H. Chen, F. Xu, A dual fitting algorithm for modal parameters identification, Mech. Syst. Signal Process. 17 (2003) 713–721.

[32] K.A. Petsounis, S.D. Fassois, Parametric time-domain methods for the identification of vibrating structures—a critical comparison and assessment, Mech. Syst. Signal Process. 15 (2001) 1031–1060, https://doi.org/10.1006/mssp.2001.1424.

[33] W.J. Staszewski, Identification of damping in MDOF systems using time-scale decomposition, J. Sound Vib. 203 (1997) 283–305, https://doi.org/10.1006/jsvi.1996.0864.

[34] M. Ruzzene, A. Fasana, L. Garibaldi, B. Piombo, Natural frequencies and dampings identification using wavelet transform: application to real data, Mech. Syst. Signal Process. 11 (1997) 207–218, https://doi.org/10.1006/mssp.1996.0078.

[35] P. Bonato, R. Ceravolo, A.D. Stefano, Time-frequency and ambiguity function approaches in structural identification, J. Eng. Mech. 123 (1997) 1260–1267, https://doi.org/10.1061/(ASCE)0733-9399(1997)123:12(1260).

[36] J.N. Yang, Y. Lei, S. Pan, N. Huang, System identification of linear structures based on hilbert–huang spectral analysis. Part 1: normal modes, Earthq. Eng. Struct. Dyn. 32 (2003) 1443–1467, https://doi.org/10.1002/eqe.287.

[37] A. Roshan-Ghias, M.B. Shamsollahi, M. Mobed, M. Behzad, Estimation of modal parameters using bilinear joint time–frequency distributions, Mech. Syst. Signal Process. 21 (2007) 2125–2136, https://doi.org/10.1016/j.ymssp.2006.09.009.

[38] J. Slavič, M. Boltežar, Damping identification with the morlet-wave, Mech. Syst. Signal Process. 25 (2011) 1632–1645, https://doi.org/10.1016/j.ymssp.2011.01.008.

[39] R.J. Kuether, M.R.W. Brake, Instantaneous frequency and damping from transient ring-down data, in: M. Allen, R.L. Mayes, D. Rixen (Eds.), Proceedings of the Dynamics of Coupled Structures, 4, Springer International Publishing, Cham, 2016, pp. 253–263.

[40] M. Hatami, M.M. Farrokhifard, V.M. Venkatasubramanian, Modal damping estimation: an alternative for hilbert spectral analysis, Proceedings of the 2019North American Power Symposium (NAPS) (2019) 1–6. October 2019.

[41] F. Sánchez Iglesias, A. Fernández López, Rayleigh damping parameters estimation using hammer impact tests, Mech. Syst. Signal Process. 135 (2020) 106391, https://doi.org/10.1016/j.ymssp.2019.106391.

[42] T.-P. Le, P. Argoul, Continuous wavelet transform for modal identification using free decay response, J. Sound Vib. 277 (2004) 73–100, https://doi.org/10.1016/j.jsv.2003.08.049.

[43] M. Boltežar, J. Slavič, Enhancements to the continuous wavelet transform for damping identifications on short signals, Mech. Syst. Signal Process. 18 (2004) 1065–1076, https://doi.org/10.1016/j.ymssp.2004.01.004.

[44] M. Mihalec, J. Slavič, M. Boltežar, Synchrosqueezed wavelet transform for damping identification, Mech. Syst. Signal Process. 80 (2016) 324–334, https://doi.org/10.1016/j.ymssp.2016.05.005.

[45] I. Tomac, Ž. Lozina, D. Sedlar, Extended morlet-wave damping identification method, Int. J. Mech. Sci. 127 (2017) 31–40, https://doi.org/10.1016/j.ijmecsci.2017.01.013.

[46] S. Hans, E. Ibraim, S. Pernot, C. Boutin, C.-H. Lamarque, Damping identification in multi-degree-of-freedom system via a wavelet-logarithmic decrement—part 2: study of a civil engineering building, J. Sound Vib. 235 (2000) 375–403, https://doi.org/10.1006/jsvi.1999.2927.

[47] J. Lardies, S. Gouttebroze, Identification of modal parameters using the wavelet transform, Int. J. Mech. Sci. 44 (2002) 2263–2283.

[48] L. Xu, Y. Deng, H. Ni, D. Sun, S. Ling, Y. Tian, Effect of aging on damping properties of rubberized asphalt binder and rubberized porous asphalt mixture, Constr. Build. Mater. 411 (2024) 134743, https://doi.org/10.1016/j.conbuildmat.2023.134743.

[49] S. Deepa, U. Saravanan, J. Murali Krishnan, On measurement of dynamic modulus for bituminous mixtures, Int. J. Pavement Eng. 20 (2019) 1073–1089.

[50] N.D. Manke, R.C. Williams, Z. Sotoodeh-Nia, E.W. Cochran, L. Porot, E. Chailleux, S. Pouget, F. Olard, A.J.D. Barco Carrion, J.-P. Planche, et al., Performance of a sustainable asphalt mix incorporating high RAP content and novel bio-derived binder, Road. Mater. Pavement Des. 22 (2021) 812–834, https://doi.org/10.1080/14680629.2019.1643769.

[51] AASHTO T-378 Determining the Dynamic Modulus and Flow Number for Asphalt Mixtures Using the Asphalt Mixture Performance Tester (AMPT); 2014.

[52] N. Hasheminejad, C. Vuye, A. Margaritis, W. Van Den Bergh, J. Dirckx, S. Vanlanduit, Identification of the viscoelastic properties of an asphalt mixture using a scanning laser doppler vibrometer, Mater. Struct. 53 (2020) 131, https://doi.org/10.1617/s11527-020-01567-9.

[53] J.D. Rodrigues, E. Freitas, J. Araújo, H. Silva, Innovative low noise surfaces-comparison of damping and absorption, Proc. Proc. 43rd Int. Congress Noise Control Eng. Inter. noise (2014).

[54] F.G. Pratico, G. Pellicano, M. Bolognese, G. Licitra, A study on frequency response functions in pavement engineering, BJRBE 18 (2023) 208–243, https://doi.org/10.7250/bjrbe.2023-18.595.
[55] J. Wang, Intrinsic damping: modeling techniques for engineering systems, J. Struct. Eng. 135 (2009) 282–291.
[56] E. Uglova, A. Tiraturyan, Calculation of the damping factors of the flexible pavement structure courses according to the in-place testing data, Procedia Eng. 187 (2017) 742–748, https://doi.org/10.1016/j.proeng.2017.04.431.
[57] C. Guo, Z. Lu, Vibration experiment of CTCP-CRCP composite pavement under heavy traffic, Int. J. Pavement Res. Technol. 12 (2019) 416–422, https://doi.org/10.1007/s42947-019-0049-5.
[58] K. Chatti, Y. Ji, R. Harichandran, Dynamic time domain backcalculation of layer moduli, damping, and thicknesses in flexible pavements, Mich. Transp. Res. Rec. (2004) 106–116.
[59] Paul S. Addison. The Illustrated Wavelet Transform Handbook: Introductory Theory and Applications in Science, Engineering, Medicine and Finance, CRC press, Boca Raton, FL, USA, 2017.
[60] P. Bonfiglio, F. Pompoli, A. Farnetani, A Simplified Method for Determining the Damping Loss Factor of Panels Using a Narrow Band Decay Method, Noise Cont. Engng J. 65 (2017) 94–102, https://doi.org/10.3397/1/376429.
[61] R. Cabell, N. Schiller, A. Allen, M. Moeller, Loss Factor Estimation Using the Impulse Response Decay Method on a Stiffened Structure. (2009).
[62] P. Yupapin, N. Pornsuwancharoen, Asphalt road surface vibration and force distribution generated by pickup truck braking, Measurement 148 (2019) 106871, https://doi.org/10.1016/j.measurement.2019.106871.